IMPACT OF HIGH PENETRATION OF PV GENERATION ON POWER SYSTEM TRANSIENT STABILITY AND FAULT CURRENT; MODELING FOR REAL-TIME STUDIES

By

Amira Abdelgadir

Abdelrahman A. Karrar
Associate Professor of Electrical Engineering
(Chair)

Ahmed H. Eltom
Professor of Electrical Engineering
(Committee Member)

Gary L. Kobet
Adjunct Professor of Electrical Engineering
(Committee Member)

IMPACT OF HIGH PENETRATION OF PV GENERATION ON POWER SYSTEM TRANSIENT STABILITY AND FAULT CURRENT; MODELING FOR REAL-TIME STUDIES

By

Amira Abdelgadir

A Thesis Submitted to the Faculty of the University of
Tennessee at Chattanooga in Partial
Fulfillment of the Requirements of the Degree of
Master of Science: Engineering

The University of Tennessee at Chattanooga
Chattanooga, Tennessee

August 2020

ABSTRACT

The electric power system is experiencing major changes in generation technology by which conventional thermal generation is replaced by with renewable energy resources RES. Over the years, many researchers investigated the effects of high injection of RES on the bulk power system. However, these studies were not in real time environment and deployed the inverter based resources in a small-scale generation levels.

This work studies the impact of high level PV injection on the synchronous generators transient stability and grid's fault current, and associated modeling as appropriate for real-time analysis. From the analysis it is found that PV generators negatively affect transient stability if they replace conventional generation. In terms of fault current, PV generators contribution to the fault current is relatively low compared to synchronous generators. The main contribution of this work will be modeling a system of PV generators that can work on real-time digital simulators environment.

TABLE OF CONTENTS

LIST OF TABLES

LIST OF FIGURES

CHAPTER 1

INTRODUCTION

1.1 Overview

The past decades have seen a transition in generation from conventional machine-based synchronous generation to Renewable Energy Resources. Such a change is largely motivated by concerns about the high greenhouse gas emissions from fossil fuel use, nuclear generation safety, and waste disposal [1] . New policies have been developed around the world for the construction of a clean energy economy. For instance, in the United States, an Executive Order that requires a minimum of 25% of the total amount of building electric energy and thermal energy should be clean energy by 2025 has been made [2] .

Renewable Energy Resources are interfaced to the grid by means of power electronic devices, hence they have completely different behavior from the conventional synchronous machines. Having high level of integration of inverter-based resources (IBRs) to the bulk power system raised many new challenges for utility engineers [3].

1.2 Problem Statement

Large integration of IBRs has raised concerns about reliability and stability of the bulk power system. The rotational inertia and the inherited damping of the synchronous machines assures system stability when a fault occurs, however, IBR has none of those features and hence make the system prone to instability in the event of faults [1]. Furthermore, IBRs do not

generally provide significant fault current as they have a controller that limits their output current. This has a major effect on protection systems that distinguish between fault conditions and normal operating conditions using fault current [4]. Hence, having high levels of IBRs could significantly alter the fault levels of the BPS and hence affect the operation of the protection system. Many researchers have studied the impacts of high PV penetration on the transient stability of synchronous generators as well as the fault current contribution from IBRs. These studies deployed the inverter based resources IBRs in a distribution system and were for small-scale generation levels.

1.3 Objective

The first objective of this work is to analyze the effects on transient stability associated with large-scale penetration of Photovoltaic, i.e up to 50% of the system total load, into the bulk power system. The second objective is to investigate the impact of high PV penetration on the fault current. The main contribution of this work will be modeling a system of PV generators that can work on real-time digital simulators environment for purposes of testing microprocessor relays using hardware-in-the-loop feature of the real time simulator.

1.4 Thesis Layout

The remainder of this thesis is organized as follows:

- Chapter II: this chapter presents the literature review.
- Chapter III: this chapter presents the methodology.
- Chapter IV: this chapter presents simulation results.

- Chapter V: this chapter concludes the contributions and findings of this work. Furthermore, it provides suggestions and recommendations for future research work.

CHAPTER 2

LITERATURE REVIEW

2.1 Short Circuit Current Analysis of IBR

2.1.1 Introduction

One of the crucial steps when designing a protection system is conducting short circuit studies to determine the required interrupting capacity of the circuit breakers which forms the basis of designing a proper relaying system. Short circuit analysis also minimizes the risk of equipment damage by ensuring rated fault current levels are not exceeded. Protection systems are designed to localize and isolate faults to prevent and minimize any unnecessary power interruption. A fault in an electrical power system is the unintentional conducting path that bypasses the normal load. The short-circuit fault is the most common one and is usually implied when the term fault is used [3].

There are mainly two types of faults that can take place on the electric grid, symmetrical and unsymmetrical faults. Symmetrical or balanced fault occurs when all three phases come into contact with each other or with the ground and this is the least common but most severe type of fault. Unsymmetrical faults include line to ground (L-G), line to line (L-L), and double line to ground (LL-G) faults. These are very common and less severe than symmetrical faults [5].

IBR injection into the generation system has raised challenges for utility engineers to assess the effects on the short-circuit strength of the network and thus the impact on switching device interruption ratings. IBR fault characteristics differ from conventional synchronous

machines. There is limited knowledge or contradictory findings about IBR 's behavior during distribution or transmission system faults because IBR's contribution to power generation could currently be considered insignificant or relatively low [3]. However, it is predicted that a rapid increase in distributed energy resources (DERs) would come online in the immediate future [3]. As the degree of IBR penetration increases, their effect on the fault current may no longer be considered insignificant, and the situation will be more complex. The level of penetration refers to the total amount of DER on a given network. It is generally obtained by dividing the IBR 's rated output power by the total load.

In this chapter the short circuit current charcteristics for both synchronous machines and inverter based resources will be discussed as well as a literature review on the impact of large scale deployment of IBRs on the available fault current.

2.1.2 Synchronous Machines Short Circuit Current

When a short circuit is applied to a synchronous machine's terminal, the current will begin very high and decline to a steady-state value. The fault current has two distinct components, a fundamental frequency component that declines at first very rapidly (in a few cycles) and then relatively slowly (in a few seconds) to a steady state value, and a unidirectional or dc offset component, that decays in an exponential manner in several cycles [5].

In general, synchronous machines deliver for several cycles about six times their rated current before decaying to slightly above rated current. During a fault, an external DC source that supplies the field current to the synchronous machine will continue to supply voltage to the field windings of the generator.Also the prime mover will keep driving the rotor which produces the desired induced voltage in the stator winding which, in effects, provides a continuous fault

current. The current value of a steady-state short-circuit will remain unless a switching device such as a circuit breaker interrupts it [5].

As a result of short circuit current flowing in the circuit, machine impedance increases due to the increase in winding temperature and this in turn will cause the AC envelope to degrade more rapidly. Three reactance variables have been standardized by the industry called the subtransient, transient, and synchronous reactance:

X_d'' = subtransient reactance; determines current during first few cycles after fault occurance and its effect lasts for about 0.1 seconds.

X_d' = transient reactance; should determine current after several cycles and its effect continues from about 0.5 to 2 seconds.

Xd = synchronous reactance; this is the value that determines the current flow after steady-state condition is reached.

Manufacturers normally provide two values for the direct axis subtransient reactance. X_{di}'' is at rated current, unsaturated, and larger than X_{dv}'' which is at rated voltage, saturated, and smaller. During a short-circuit event the generator may become saturated. So, for conservatism, the X_{dv}'' value is commonly used when calculating fault currents. To understand the reactances values, consider the characteristics of the fault current decaying envelope driven by the machine's magnetic field stored in the generator windings, which cannot change in magnitude instantaneously but rather decays over time [3]. Figure 2.1 below show the synchronous generator fault current during subtransient, tranient and steady state periods without the DC offset.

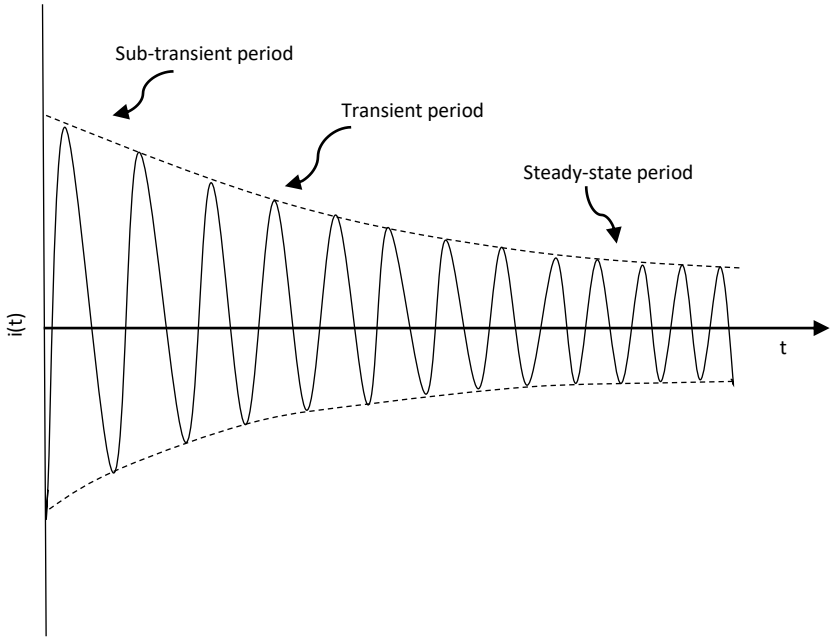

Figure 2.1

Synchronous machine response to 3-phase fault

2.1.3 Fault Characteristics of Inverter-Based Resources

The dynamic behavior of inverter based resources totally differ from synchronous machines and this is due to the fact that they are connected to the grid by means of power electronic inverters. Inverters do not develop the required inertia and damping to carry fault current based on an electro-magnetic characteristic since they not have a rotating mass component. Power electronic inverters lack predominately inductive characteristics that are associated with rotating machines, therefore, they have a much faster decaying envelope for fault currents. On the other hand, unlike rotating machines, inverters can be controlled and programmed in a manner that make them able to vary the length of time taken to respond to fault conditions. During transient situations,the DC link capacitor between the DC/AC converter and

the IBR unit keeps the voltage near constant. This will also reflect on the fault current characteristics of inverters [3].

The inverter controller that controls the inverter normally uses one of two control schemes, a voltage control scheme or a current control scheme. In terms of fault current magnitude and decaying time constant,the voltage control scheme has higher initial current overshoot compared to the current control scheme which has a much slower intial increase and decay back to steady-state values.Therefore, during the transient period the fault contribution will be higher if the IBR's inverter is under the voltage control scheme [6].

The type of IBR that is used in this study is the Solar Photovoltaic. During a short circuit fault taking place on the grid, the PV system feeds the short circuit current current but its contribution depends on the PV inverter design. During normal operating conditions the PV systems are modeled to provide the maximum power available from PV panels to the system; the PV inverter attempts to push this power even under low voltage conditions assosiated with the fault, i.e., it will try to behave like a constant power source. Hence, the current injection from a PV inverter to the system can be given by $I = P_{PV}/V$, where P_{PV} is the power from the PV panels and V is the ac terminal voltage. If this current exceeds the maximum current rating of the inverter the inverter is required to limit its fault current injection, in order to protect the electronic devices. This is done by reducing the internal voltage during the short circuit. Inverters limit their current to one to two times the rated current [7]. This reduction in the fault current capacity of inverters may result in protection problems, because over-current based conventional protection schemes are not employed to detect such low fault currents.

Phase voltages of three phase inverters during fault may include: (1) only positive sequence component, or (2) positive and negative sequence components, or (3) positive, negative

and zero sequence components depending on configuration of the inverter and fault type [5]. In order to determine the short-circuit current characteristic of an inverter, testing needs to be conducted. These test results can be used to design IBR inverter models that can be used in distribution models.

2.1.4 Prior Research on Inverter Based DER Fault Current

There are very few references that show actual fault currents from IBR, but there are some articles that have discussion on this topic. A number of IBR short circuit current research has adopted a "rule of thumb" of one to two times an inverter's full load current for one cycle or less [8] [9].

In 1985 and 1986, thirty 2-kW PV static power converters were installed on one phase at the end of a 13.8-kV feeder by New England Electric in Gardner, Massachusetts. Extensive testing has been conducted by the utility to see if the static power converter could reliably detect island conditions and faults in the presence and absence of a utility source. During the experiment, inverters were shown to contribute a small current transient during faults. The fault current injection from the inverters was less than 200% rated peak inverter current and had a duration less than 200 microseconds. Thus the inverters were considered to have no or negligble impact on the intensity or duration of the fault and also did not affect the feeder protection systems [10].

In the study of the Gardner Test Site feeder projected for the year 2018, the 3 MW of projected inverter installations distributed around the feeder did not impact the fault calculations or fuse sizing as long as the fuses were rated for the generating current of the inverters as well as the feeder loads. The inverters at the Gardner Test Site would not provide any current to a fault

after one-half cycle. Inverters in general might provide sustained fault current less than 150 percent rated current to a fault, which may be considered a negligible fault contribution [10].

GE, in their report, "DG Power Quality, Protection, and Reliability Case Studies" found that voltage regulation can be a major problem for DER penetration levels of 40% [11]. The sudden loss of DER, specifically as a result of false tripping during voltage or frequency events, can result in excessively low voltages in parts of the system. In terms of fault current, GE assumed that inverter-based DER did not contribute significantly to fault currents, the DER did not adversely affect the ratings of the fuse and circuit breakers. However, the studies also pointed out this could not be the case when the DER is tied a point where the utility source impedance is unusually high, i.e,weak system. The results also indicated that, at higher IBR penetration levels, it may be beneficial for inverters to have the capability to ride through system faults.

NREL has conducted a short-circuit test for a 1 kW, single phase inverter and the maximum measured peak fault current was almost 5 times the steady-state normal current [3]. Similar testing was conducted at an inverter manufacturer's facility using a larger inverter, a 500 KVA 3-phase inverter. The manufacture inverter fault current was approximately 2 to 3 times the rated peak output current. Both inverters test results suggest that inverters designed to meet IEEE 1547 and UL 1741 produce fault currents anywhere between 2 to 5 times the rated current.

It was pointed out in [12], that the effect of a single small DG unit on the fault current may be insignificant; however, the cumulative contributions of many small units, or a few larger units, can adjust the short-circuit levels enough to cause protective devices to malfunction. Higher fault currents will especially affect the Reclosers (RC) on the feeder. For example, extra fault current from an upstream DG may exceed maximum interrupting current limit of one or more RCs, possibly resulting in mechanical and/or thermal damage. Extra fault currents from

DGs will also influence the fuse operation, as they will cause the fuses to clear sooner than designed. This may cause Recloser-fuse miscoordination and thus effect the feeder's reliability noticeably [12] [13].

The author of [14] investigated the impact of high penetration of DGs on existing protection schemes. The UK generic distribution network which contain a 33/11.5 kV substation was used for simulations, whereby relays were configured, and DGs were added, and their performance was tested under fault conditions using DIgSILENT PowerFactory software tool as the main simulation platform. Three fault scenarios along the feeder were conducted and the fault level was obtained from the simulation with and without the presence of the Photovoltaic DG where a decrease in line current levels is observed when faults occurs with DGs in the network. Additionally, it is noticed that the voltage and frequency profiles match closely. It was concluded that the small-scale DG penetration requires no amendments for relay coordination parameters. But the study projected that large-scale DG penetration would require parameters of protective devices to be adjusted due to fluctuating frequency as well as significant fault current contribution.

The author of [15] performed a comprehensive study on IEEE 30-Bus test system to address the impacts of high PV and wind penetration into the grid. The integration of DG plants into the 33kV distribution network was implemented using Etap software. The total system load was 300 MW, three levels of DG penetration were modeled, 15%, 30% and 50% and 3 buses were selected to be faulted by 3-phase short circuit fault individually to investigate the impact on the grid and fault level at each level of penetration. It has been found that the fault current increased in all buses, accordingly rising the fault level. Thus, the study suggested that proactive measures should be taken to eliminate the effect of such significant rise on the 3-phase fault

current and its impact on the grid apparatus and equipment. The research has concluded that the optimum level of DG integration for the today's grid is 30%, while higher level of integration requires a mitigation measure of the DG impact illustrated in the study, as well as, grid configuration. The results obtained in [15] are in line with the recommendation published by IRENA in 2013 [16] when it stated that, if the level of DG penetration exceeded 30% the implementation of the Smart Grid become necessary.

The author of [17] investigated the effect of increase in fault current with increased penetration of PV systems in residential power supply networks modeled in s PSCADA software environment, where a PV unit has been installed in all of the 14 residences. In the model the PV system was modeled as a voltage source that can contribute about 50% the power requirement for the 5kVA load. A three phase fault was applied at 4 different locations and one single line to ground fault was also applied. During a fault at the main distribution board the fault current contribution from the PV system is limited to a value of 1.5 times of inverter full load current. The research illustrated that even though individual PV system installed in residences might not contribute enough fault current to be able to make an impact on the fault interruption capacity of switching device, multiple PV units connected to the network will make cumulative contribution to the point of fault and thus affect the ability of switching device to clear fault. An important factor to consider and analyze is the duration for which the PV system can contribute to the fault. This has a significant impact on the fault withstand capacity of the short circuit protection device as well as the downstream bus bar system.

All the previous research studied the effect of high PV peneteration on the fault current, however, the capacity of the IBR under study ranges from few kilowatts to few megawatts which is considered a relatively low capacity compared to the dominant synchronous machines. In

addition, most of these studies had IBR that deployed in a distributed manner. In this work the effect of high PV penetration on a multi machine system will be simulated in real time using RT-Lab RTDS along with Matlab/Simulink. The PV panels will be modeled as a single PV generator, not as distributed resources, that have a very high capacity up to 500MW.

2.2 Effect of High PV Penetration on Transient Stability

2.2.1 Introduction

Power system stability can be defined as the ability of a power system to stay in a state of equilibrium during normal operating conditions and to recover an acceptable state of equilibrium when subjected to disturbance. Conventionally, the stability main concern has been of maintaining synchronous operation. Since electrical power generation is dominated by synchronous machines, a crucial condition for acceptable system operation is that all synchronous machines should remain in synchronism. Maintaining synchronism between synchronous machines is affected by the dynamics of generator rotor angles and power-angle relationships.

Instability is not always linked with the loss of synchronism but it could rather be encountered when the voltage of the load collapsed. In this case, remaining in synchronism will not be an issue but maintaining the stability and control of the voltage [5]. System stability is evaluated by the power system behavior when subjected to a transient disturbance, either small or large. Load change is a type of small disturbance that occurs frequently in the power system, and normally the system adjusts to these changes and also continues supplying the maximum load. The system should also be able to withstand severe disturbances such as a short circuit, loss of generator or load, or loss of a tie between two interconnected systems.

The system response to a severe disturbance goes beyond not only affecting the equipment. For instance, a short-circuit on a critical element followed by its separation by protective relays will also influence power transfers, machine rotor speeds, and bus voltages; the voltage deviations will actuate both generator and voltage regulators; the speed deviations will actuate the governors; the variations in voltage and frequency will affect loads on the system in different ways depending on their individual dynamics. Moreover, protection devices may respond to deviations in system variables and thus affect the system reliability [5]. In order to simplify the problem, many assumptions are usually made to focus on factors affecting the particular type of stability problem. The understanding of stability problems is greatly facilitated by classifying the stability into various categories.

2.2.2 Classification of Stability

The classification of power system stability proposed here is based on the following considerations [5]:

- The physical nature of the resulting mode of instability.
- The size of the disturbance considered which influences the method of calculation and prediction of stability.
- The devices, processes, and time span that must be taken into consideration in order to assess stability.

Figure 2.2 identify power system stability categories and subcategories.

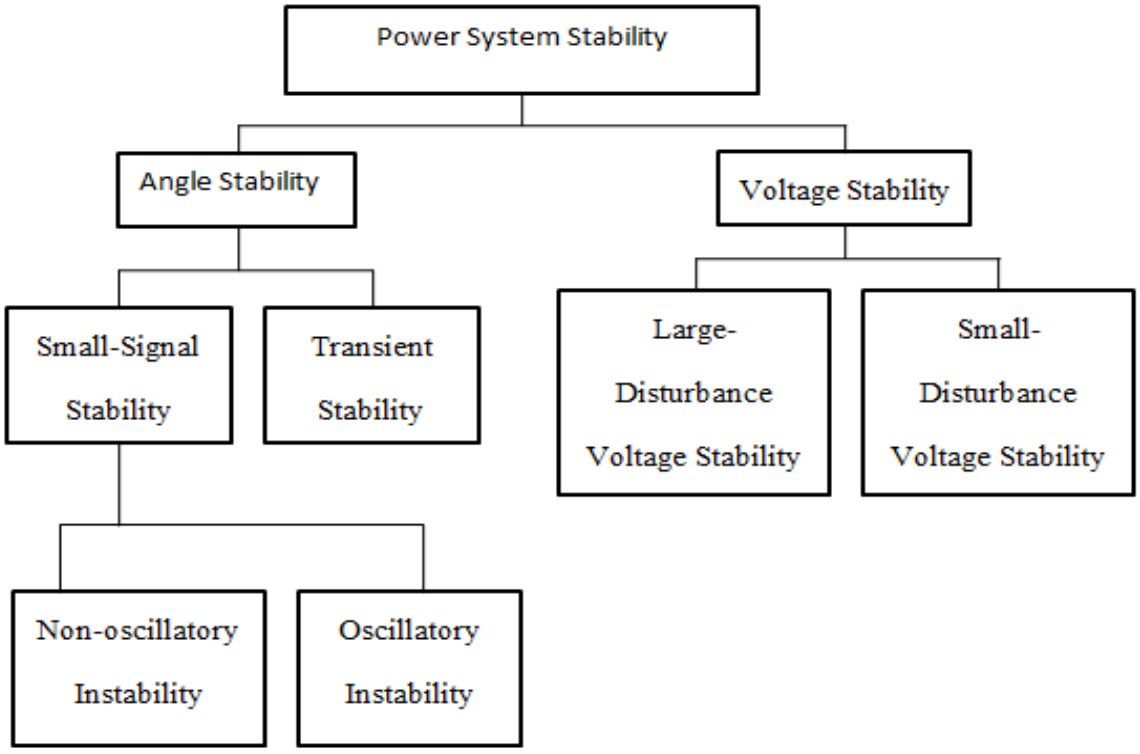

Figure 2.2

Categories of Power System Stability

2.2.2.1 Voltage stability

IEEE/CIGRE Task Force define voltage stability as: "Voltage stability is the ability of a power system to maintain steady voltages at all buses in the system after being subjected to a disturbance from a given initial operating condition". Voltage stability events have a duration that ranges from a few cycles to minutes. Based on this time span, voltage stability can be divided into transient voltage stability and long-term voltage stability. The time frame of

transient voltage stability is zero to ten seconds, while the time frame of long-term voltage stability is often several minutes [5].

A power system may be subject to voltage instability when a disturbance, an increase in load demand or alteration in system state leads to a progressive and uncontrollable drop in system voltage [5]. Voltage stability is highly influenced by transmission system characteristics, generator characteristics and load dynamics.

IEEE/CIGRE Joint Task Force defines voltage collapse as "the process by which the sequence of events accompanying voltage instability leads to a blackout or abnormally low voltages in a significant part of the power system" [18]. According to Hill et al, in their set of stability definitions [19] voltage collapse is "a power system at a given operating state and subject to a given large disturbance undergoes voltage collapse if it is voltage unstable or the post-disturbance equilibrium values are nonviable". In severe conditions, voltage collapse could result in a blackout.

2.2.2.2 Rotor angle stability

When connecting two or more synchronous machines, all stator voltages and currents for the machines must have the same electric frequency and the mechanical speed of the rotor of all machines should be synchronized to this frequency. Therefore, the rotors of all interconnected synchronous machines must be in synchronism. Rotor angle stability is defined as "the ability of interconnected synchronous machines of a power system to remain in synchronism" [5].

2.2.2.2.1 Power versus angle relationship

Assuming the voltage magnitude of the source and load are held constant, and the load voltage angle is fixed at 0 for a lossless line of reactance X, the power delivered to the load is given by the following equation

$$P_L = \frac{E_s V}{X} \sin \delta \qquad 2.1$$

As shown in figure 2.3 the active power varies as a sine of the angle; a highly nonlinear relationship. When the angle is zero, no power is transmitted. When the source angle increases, the active power transmitted to the load also increases, till the angle it reaches its maximum, nominally 90˚, after reaching its maximum any further increase in angle will result in a decrease in the load power.

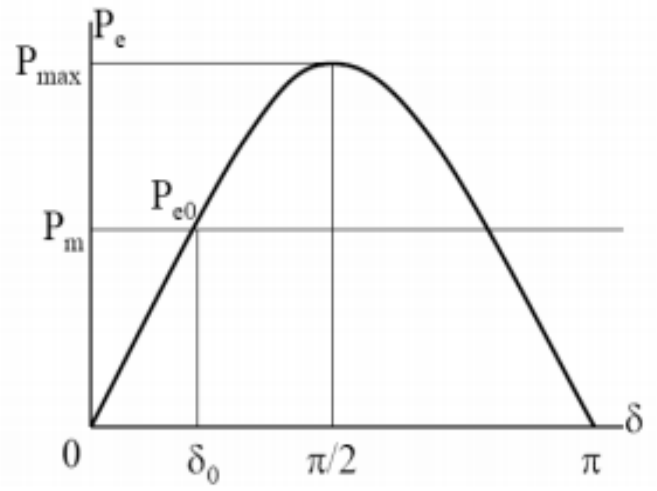

Figure 2.3

Power-Angle Relationship

2.2.3 The stability phenomena

Stability is a condition of maintaining equilibrium between two or more opposing forces. Interconnected synchronous machines maintain synchronism with one another by restoring forces, which takes an action whenever one or more machines start to accelerate or decelerate with respect to other machines by means of external forces. During steady-state conditions, there is equilibrium between the input mechanical torque and the output electrical power of each machine, and the speed remains constant. If the system is disturbed this equilibrium is also disturbed, driving machines rotor to accelerate or decelerate according to the laws of motion of a rotating mass. lf one generator temporarily runs faster than another, the angular position of its rotor relative to that of the slower machine will advance. The resulting angular deviation allocate part of the load from the slow machine to the fast machine, depending on the power-angle relationship. This tends to reduce the speed difference and hence the angular separation. The power-angle relationship as mentioned above is highly nonlinear. After a certain limit, any increase in angular deviation will result in a decrease in power transfer; in return, this increases the angular separation further and leads to instability. For any given situation, the stability of the system depends on whether or not the variations in angular positions of the rotors will provide enough restoring torques [5].

When a synchronous machine loses synchronism or "falls out of step" with the rest of the system, its rotor turns at a higher or lower speed and fails to generate voltages at the required system frequency. The "slip" between rotating stator field (synchronized to system frequency) and the rotor field leads to large oscillations in the machine power output, current, and voltage; this may trigger some protection systems to separate the unstable machine from the system [5].

Generally, rotor angle stability is divided into two categories:

(a) Small-signal stability: is the ability of the power system to maintain synchronism under small disturbances. Such disturbances take place frequently on the system because of small deviations in loads and generation. Instability that may occur have one of two forms: (i) steady increase in rotor angle because of the lack in the required synchronizing torque, or (ii) rotor oscillations of increasing magnitude due to lack of the required damping torque. The way in which the system responds to these disturbances depends on the initial operating conditions, the transmission system strength, and the type of generators exciter used.

(b) Transient stability is the ability of the power system to maintain synchronism when subjected to a severe transient disturbance. The associated system response involves large excursion of generator rotor angles and is influenced by the nonlinear power-angle relationship. Stability depends on both the initial operating conditions of the system and the degree of the disturbance [5].

Disturbances of wide range of severity and probability of occurrence can take place on the power system. However, the system should be designed to have the ability to be stable for a number of contingencies. The contingencies generally considered are short-circuits of different kinds that normally assumed to occur on transmission lines, but sometimes bus or transformer faults are also considered. The fault is cleared by actuating the relay which operates the appropriate circuit breaker to opens its contacts and isolate the faulted parts. In severe cases, high-speed reclosure may also occur which can exacerbate the problem for permanent faults.

Figure 2.4 shows the behavior of a synchronous machine's rotor angle for three conditions; one stable case and two unstable cases. In Case 1, the stable one, the rotor angle increases to a maximum, then decreases and oscillates with decreasing magnitude until it reaches a steady state. ln Case 2, the rotor angle continues to increase gradually (drifting) until the

machine loses synchronism. This type of instability is called first-swing instability and is caused by lack of synchronizing torque. In Case 3; the system is able to remain stable in the first two swings and after that becomes unstable as a result of developing oscillations when approaching the end state. This kind of instability normally occurs when the post fault steady-state condition itself is undergoing a small-signal disturbance, and not necessarily as a result of the transient disturbance [5].

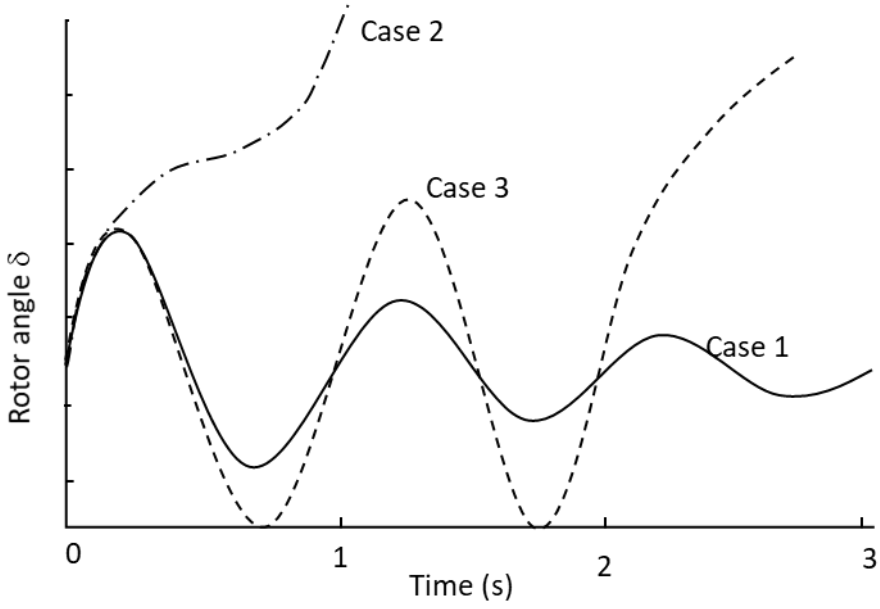

Figure 2.4

Rotor angle response to a transient disturbance

In large power systems, transient instability may not always occur as first- swing instability; it could be the result of the accumulation of several modes of oscillation causing large excursions of rotor angle beyond the first swing. ln transient stability studies the period of interest is the first 3 to 5 seconds after the disturbance, and for very large systems it may extend to about ten seconds.

2.2.3.1 Response to a short circuit fault

A three-phase fault is applied at location F for the system shown in figure 2.5.a The corresponding equivalent circuit for the faulted system, assuming the classical generator model, is shown in Figure 2.5.b The fault is cleared by opening circuit breakers contacts at both ends of the line, and the fault- clearing time depend on the relay time and breaker time. If the fault location F is at the sending end (HT bus) of the system, no power will be transferred to the infinite bus. Neglecting generator and transformer resistances, the short circuit current path from the generator to the fault location have only pure reactances. Hence, only reactive power flows and the active power P transmitted will be zero during the fault. If the fault occurs at a location F, which is at some distance away from HT bus as shown in Figures 2.5.a and b, some active power is transferred to the infinite bus during the fault.

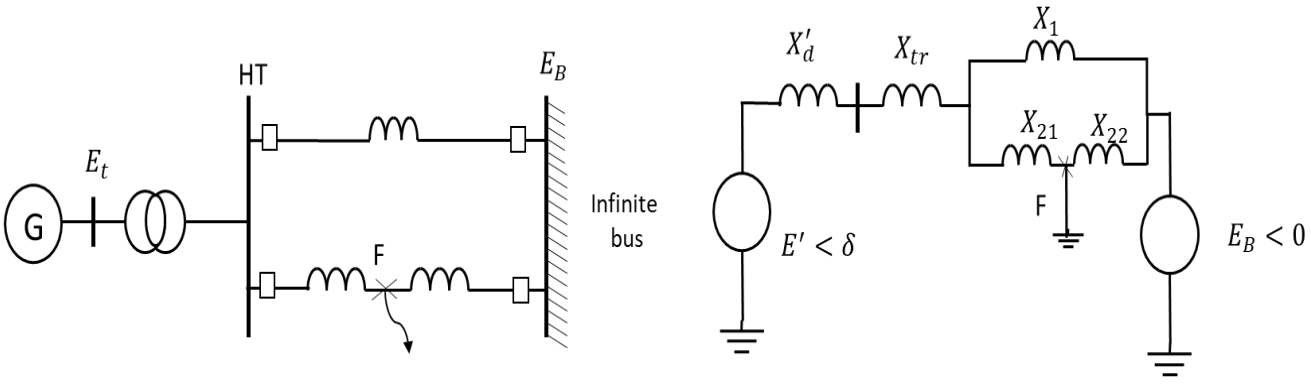

Figure 2.5

Synchronous machine connected to an infinite bus
(a) Single line diagram (b) Equivalent circuit

Figures 2.6.a and b represent the power and rotor angle plots for the three conditions: (i) pre-fault (normal operating condition), (ii) during a three-phase fault at location F shown in Figure 3.4.a, and (iii) post-fault (after isolating the faulted line). Figure 2.6.a illustrates the system response with a fault-clearing time of t_{c1} and represents a stable case while Figure 2.6.b considers a longer fault-clearing time of tc_2 such that the system is unstable. In both cases the mechanical power P_m supplied to the generator is constant.

Consider the stable case described by Figure 2.6.a. At first, both circuits are in service and the system is balanced such that electrical power $P_e=P_m$ and $\delta=\delta_0$. When the fault occurs, the operating point abruptly changes from a to b. due to inertia, angle δ cannot change instantaneously. Since P_m is now greater than P_e the rotor accelerates until the operating point reaches c, when the fault is cleared by tripping circuit 2 out, the operating point now suddenly moves to d. Now P_e is greater than P_m, driving the rotor to decelerate. The rotor angle δ continues to increase as long as the rotor speed is larger than the synchronous speed ω_0 until the kinetic energy gained during the period of acceleration (represented by area A1) is consumed by transmitting the energy to the system. The operating point moves from d to e, such that area A2 is equal to area A1. At point e, the speed is equal to ω_0 and δ has reached its maximum value δ_m. Since P_e is still greater than P_m the rotor continues to slow down, with the speed falling below ω_0. The rotor angle also decreases, and the operating point retraces the path from e to d and follows the power-angle curve for the postfault system farther down. The minimum value of δ is such that it satisfies the equal-area criterion for the postfault system. If there is no source of damping, the rotor continues oscillating with constant amplitude [5].

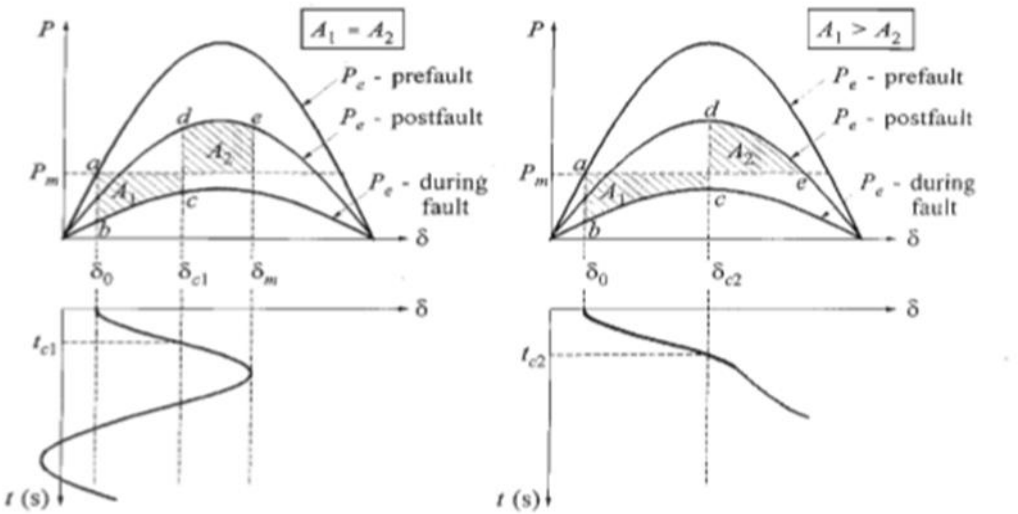

(a) Stable Case (b) Unstable Case

Figure 2.6

Illustration of transient stability phenomenon

With a delayed fault clearing time of t_{c2}, as shown in Figure 2.6.b, area A2 above P_m is less than A1. When the operating point reaches e, the kinetic energy acquired during acceleration has not yet been completely consumed; therefore, the speed is still greater than ω_0 and δ continues to increase. Beyond point e, P_e is less than P_m, and the rotor starts to accelerate again. The rotor speed and angle continue to increase, resulting in loss of synchronism.

2.2.4 Factors affecting transient stability

Transient stability of synchronous generators depends on the following factors [5]:

- The generator's loading when the fault occurs.
- The generator output during the fault, which depends on the fault location and type.
- The fault-clearing time.
- The postfault transmission system reactance.
- The generator reactance; a lower reactance increases peak power and reduces initial rotor angle.
- The generator inertia. The higher the inertia, the slower the rate of change in angle. This reduces the kinetic energy gained during fault; i.e., area A 1 is reduced.
- The generator internal voltage magnitude (E'). This depends on the field excitation.
- The infinite bus voltage magnitude E_B.

2.2.5 Critical clearing time

The ability of a generator to return to a steady state when subjected to transient disturbance like faults is significantly influenced by the fault clearing time. Relatively long fault clearing time would lead to loss synchronism and the system will become transiently unstable. The maximum amount of time to clear a fault without losing synchronism is called the "critical clearing time". This critical clearing time when compared to the expected clearing time, indicates the margin of safety between stability and instability [5]. On the 60 Hertz bulk power systems, faults are often cleared in six cycles or less. If it's assumed that the critical clearing time for a specific three phase fault is ten cycles, then margin of safety in this case will be four cycles. Small safety margin designates a crucial situation. Determining the critical clearing time and

margin of stability for all systems' machines is a crucial step when conducting stability studies. CCT depends mainly on the machine's inertia, initial operating conditions and the severity of the fault.

2.2.6 Prior Research on Impact of High IBR Penetration on Stability

The total or partial replacement of synchronous machines with IBR would negatively affect transient stability due to the lower system inertia and the higher generator reactance. The inherent rotational inertia of the synchronous machines and the damping provided by governors assures system stability in the event of faults such as loss of generators, sudden fluctuation in power injections due to variable renewable sources, tie line faults, system splits, loss of loads, etc. In case of a frequency deviation, the inertia of synchronous machines acts as a first response by providing kinetic energy to the system (or absorbing energy). In contrast, converter interfaced generation fundamentally offers neither of these services, thus, making the system prone to instability.

The author of [20] used PSCAD/EMTDC to study the impacts of high PV penetration on the transient stability of a 1000 MVA synchronous generator (SG) connected to an infinite bus through a transformer and a double circuit transmission line. Three phase fault was applied near the SG and several scenarios in terms of levels of PV penetration, operation method of the conventional generator and existence of low voltage ride through (LVRT) capability were considered. It was concluded that the transient stability is better for the scenarios of the higher penetration PV without LVRT capability and the operation of SG with fixed capacity. Ref [21] reached the same conclusion; that dividing generation between conventional power plants and large renewable energy resources (RES) and small scale distributed generation (DG) units

improves power system transient stability and enhances the network's capability in handling larger disturbances.

Ref [22] has investigated the transient stability of a two synchronous machine power system without PV and with four levels of PV penetration (10%, 20%, 30% and 40%). The Photovoltaic generator was connected to the two-machine system at the middle bus and Matlab/Simulink simulation software was used to find the CCT for each case when applying a three phase fault. Simulation results showed that until certain PV penetration level (up to the 30%) the power system transient stability is enhanced. However, the negative effect was found on higher penetration (40%) level.

In [23], the transient stability of IEEE 14 bus system with high penetration of RES that varies from 0 to 100% was investigated in Matlab/MATPOWER using Cutset Index and Improved Cutset Index as a measure for system stability. The results showed that the penetration of RES does influence the system stability, and their impact depends on the penetration level and the allocation of RES. However, given the specific network topology and parameters, the exact threshold of the highest penetration level as well as the optimal RES allocation still need further exploration.

In [24], a Texas 2000-bus case with high-PV penetration levels has been used to conduct transient stability analysis. The study demonstrated that replacing critical rotating-type synchronous generators with static PVs could bring in negative stability impacts to the network especially in case of high-PV penetration levels. The authors of [25] and [26]_ came up with the same conclusion using IEEE 9 bus system that turning from traditional generation to distributed generation causes considerable loss of overall system inertia which leads to loss of stability of the system and that the system stability depends on the location of the DER.

CHAPTER 3

METHODOLOGY

3.1 Introduction

The studies in this work are all performed on a test system provided by IEEE called D29 system, which represents one of IEEE systems that are used by Power System Relaying & Control Committee (PSRC), one of Power and Energy Society (PES) committees. This system was created by the D29 working group, whose assignment is to create a tutorial on setting impedance-based power swing blocking and out-of-step tripping functions related to transmission line applications. The system was originally modeled by the PSRC working group in PSS/E and in this work it is simulated and modelled using the RT-Lab real-time digital simulator. The model is developed in MATLAB/Simulink® which is compatible with RT-Lab platform. The system basically consists of sixteen buses, five generators, two equivalent sources generators, five two winding transformers, two three winding transformers and nine loads. Figure.3.1 shows the single line diagram of the system.

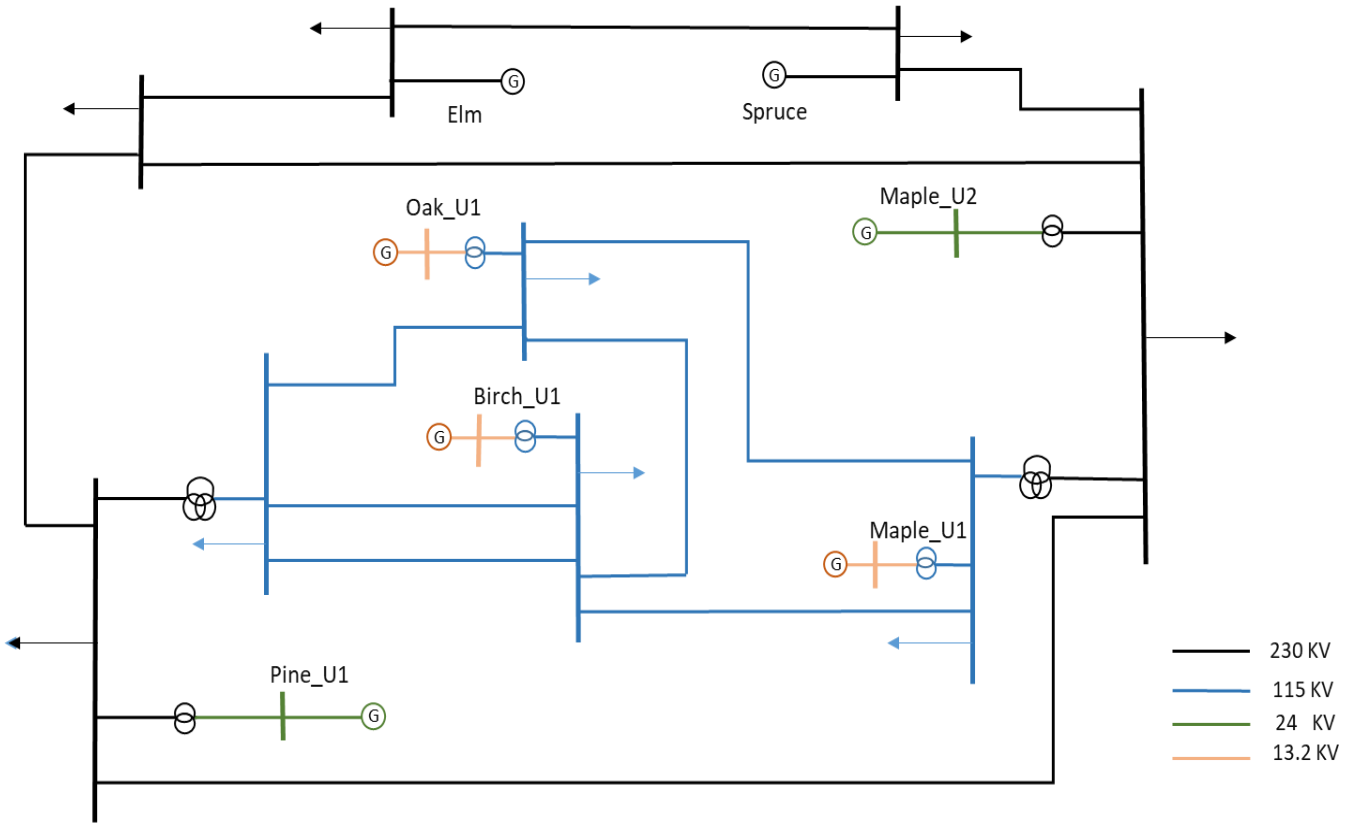

Figure 3.1

D-29 system

3.2 Generators Modeling

The generators were modeled by the three-phase round-rotor synchronous machine from Simscape library. The machines take the mechanical power P_m and the field voltage V_f as inputs and output the three phase currents. The electrical part of the machine is represented by a sixth-order state-space model. The model takes into account the dynamics of the stator, field, and damper windings. The equivalent circuit of the model shown in Figure 3.2 is represented in the rotor reference frame (q-d frame). All rotor parameters and electrical quantities are viewed from

the stator. They are identified by primed variables. Field and damper windings parameters (resistances, leakage inductances, and mutual inductances) are all entered in pu.

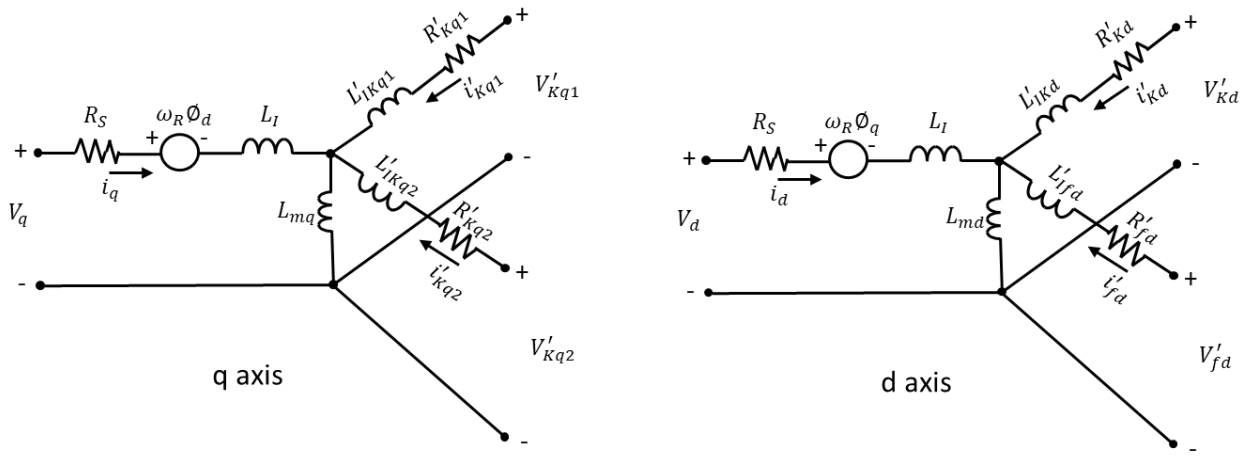

Figure 3.2

Synchronous machine model in the d-q axis

Where:

d, q — d- and q-axis quantity

R, s — Rotor and stator quantity

l, m — Leakage and magnetizing inductance

f, k — Field and damper winding quantity

One of the limitations of this model appears in discrete systems; when discretizing the Synchronous Machine block with the trapezoidal non-iterative solver, a small parasitic

resistive load should be connected at the machine terminals, to avoid numerical oscillations. Large sample times require larger loads. The minimum resistive load is proportional to the sample time. As a rule of thumb, with a 25 μs time step on a 60-Hz system, the minimum load is approximately 2.5 percent of the machine nominal power. For instance, a 300 MVA synchronous machine in a power system discretized with a 50 μs sample time requires approximately 5 percent of resistive load or 15 MW. If the sample time is reduced to 20 μs, a resistive load of 6 MW would be sufficient. However, if the Synchronous Machine block is discretize using the trapezoidal iterative (alg. loop) solver, a negligible parasitic load that is less than 0.1% of the machine MVA could be used while preserving numerical stability but this iterative model produces an algebraic loop which results in a slower simulation speed [27].

In this work, the model runs in discrete simulation type using a fixed size step of 50 μs, to avoid the numeric oscillation, all machines were discretized using the trapezoidal non-iterative solver and a negligible load of 0.5% of each machine MVA was connected at the machine terminals and the model runs stable without any numeric oscillation. Five generators have a governor and exciter and the two equivalent sources were remodeled as equivalent sources.

3.3 Exciters

The SG has fundamentally two inputs: a mechanical power input to drive the rotor and a DC input to the field winding responsible for generating the field flux. The excitation system function is to regulate and supply the DC input to the rotor circuit to obtain the required voltage performance [25]. The fundamental aim of the excitation system is to control the field current according to the change in the SG output power to maintain a steady terminal voltage. Moreover,

the excitation system improves system performance during transient conditions. The main components of the excitation system are:

- Voltage transducer.
- Exciter.
- Amplifier or regulator.
- Power System Stabilizer (PSS).
- Limiters.

The synchronous machine's terminal voltage is continuously sensed by the voltage transducers; this voltage is then filtered and rectified to DC. The DC voltage is compared to the reference voltage supplied to the exciter and the difference between them is compensated and regulated by the voltage regulator. After the amplification of the error signal, it is sent to exciter whose output is fed to the field windings.

The PSS provide an auxiliary stabilizing signal to enhance the transient performance of the system. Under excitation and over excitation limiters are control logics that keep various system parameters such as the field current, terminal voltage, and field voltage within their allowed limits. Thus, it protects the excitation and the synchronous generator system from damages [28].

In the D29 system used here PSS and limiters have been neglected and three types of exciters were used:

3.3.1 IEEEX1, Figure 3.3

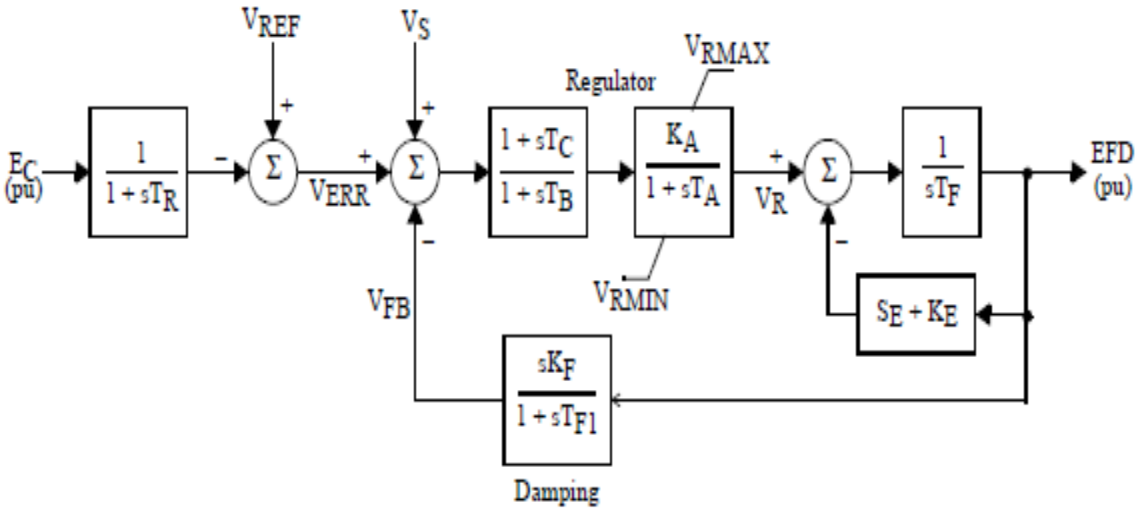

Figure 3.3

IEEEX1 exciter model

This exciter was used with both Maple U1 and Oak generators.

3.3.2 ST4B, Figure 3.4

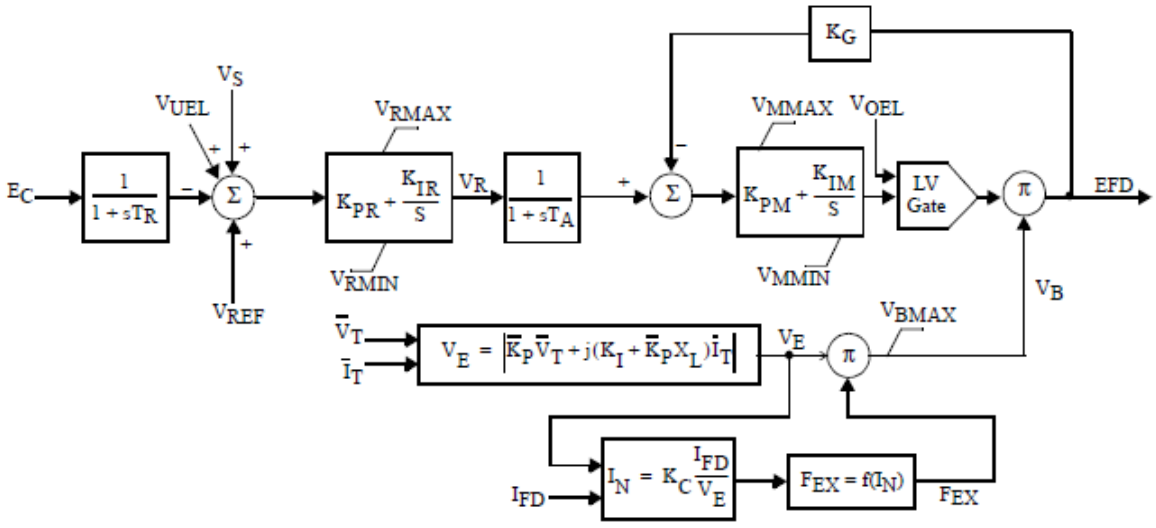

Figure 3.4

ST4B exciter model

This exciter was only used with the generator at Birch.

3.3.3 EXAC1, Figure 3.5

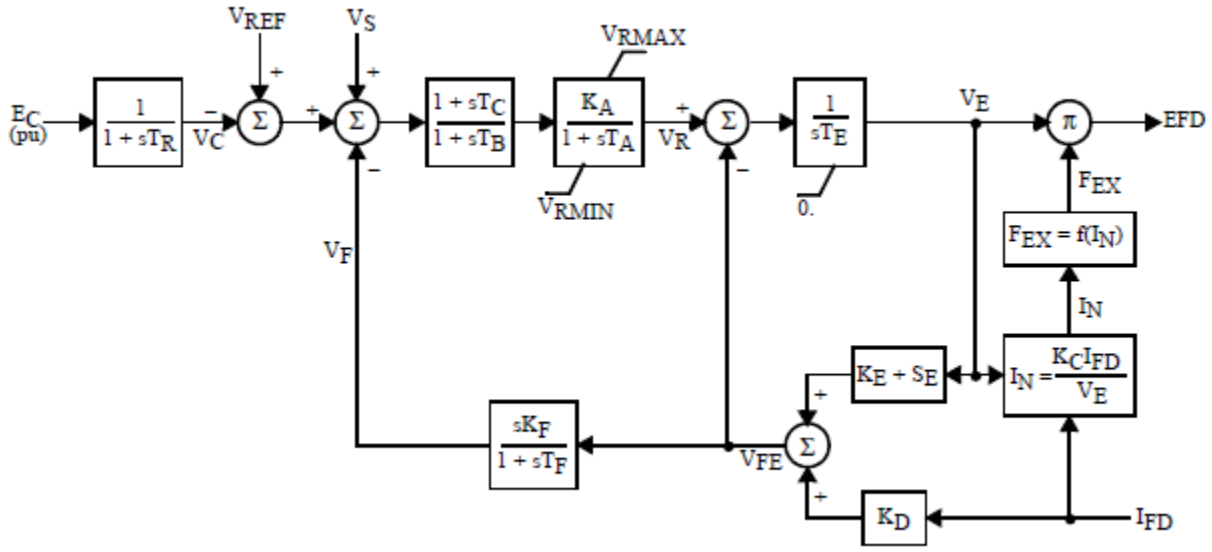

Figure 3.5

EXAC1 exciter model

This exciter was used at both Maple U2 and Pine units.

3.4 Turbine-governor system

The input mechanical power is supplied to the SG by means of prime movers. The synchronous generators convert this mechanical power to electrical power. In a thermal generating plants, boilers and turbines together establish the prime mover section [29]. Boilers burn fossil fuels like coal and gas to produce high pressure and high-temperature steam. This steam is then used by a steam turbine to provide rotating energy to run the rotor of the SG. Hydraulic turbine, on the other hand uses the potential and kinetic energy of water to produce the

rotational energy [30]. Electric torque and rotor speed of the SG change depending on the load demand which continuously changing, this change in the speed leads to frequency deviation. The function of the governor system is to control this phenomenon by regulating the mechanical input power to the SG to control its electrical output to maintain the load-generation balance [29]. Since the frequency of the system is related to the output speed of the rotor shaft, a change in the load can be seen as a deviation in the rotor speed. A governor system identifies this deviation in the rotor speed and modifies the power input to the SG to obtain the desired frequency. In the case of parallel operation of generators, power sharing is enabled by providing a droop control mechanism [30]. In this thesis, two models of turbine governor system were used:

3.4.1 Gas turbine-governor model GAST, Figure 3.6

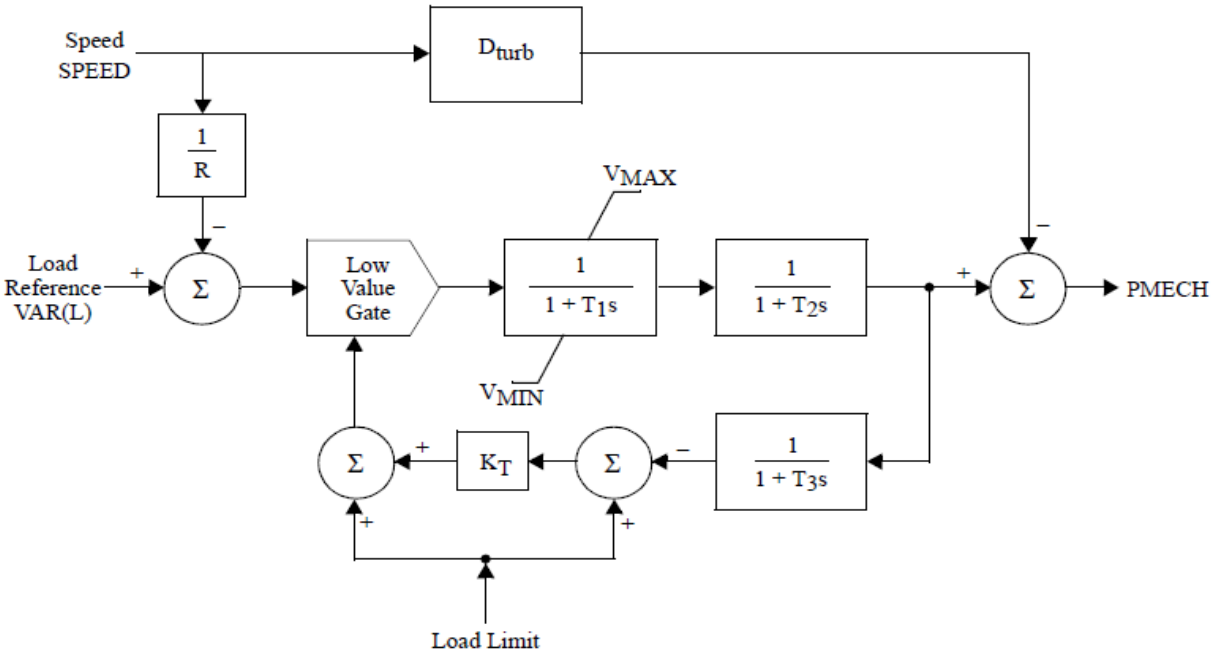

Figure 3.6

GAST governor model

This model was used with each of Birch, Maple U1 and Oak units.

3.4.2 IEEE Type 1 Speed-Governing Model IEEEG1, Figure 3.7

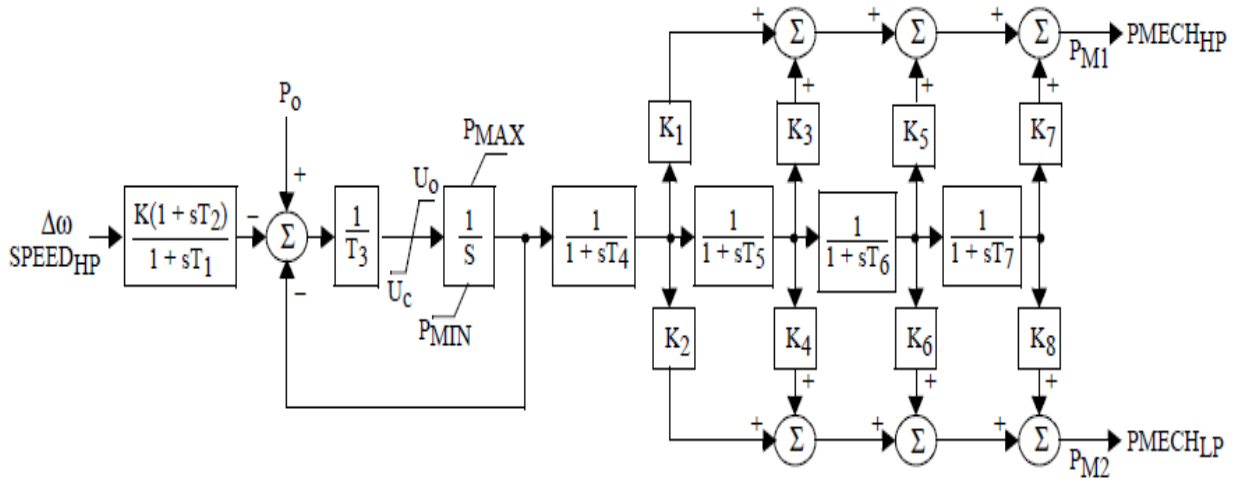

Figure 3.7

IEEEG1 governor model

This model was used with both pine and Maple U2 units.

3.5 Transmission line and load Models

A three-phase transmission line PI section was used to implement the system transmission lines. The model consists of one set of RL series elements connected between input and output terminals and two sets of shunt capacitances lumped at both ends of the line as shown in Figure 3.8.

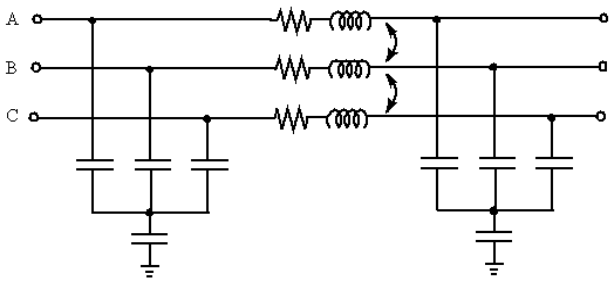

Figure 3.8

Transmission lines model

The line parameters R, L, and C are specified as positive- and zero-sequence parameters that take into account the inductive and capacitive couplings between the three phase conductors, as well as the ground parameters. This method of specifying line parameters assumes that the three phases are balanced.

The load considered in this work is a balanced three-phase load that has a constant active power and zero reactive power.

3.6 Photovoltaic System Model

A solar photovoltaic system (a PV system) is a renewable energy source, which converts the solar irradiance from the sun into electrical energy. The main components of the PV system are:

- Solar PV array module
- dc-dc boost converter
- Inverter
- Inverter control system

In this work, the model used for PV system is the average model provided by Matlab/Simulink and its single line diagram is shown in Figure 3.9.

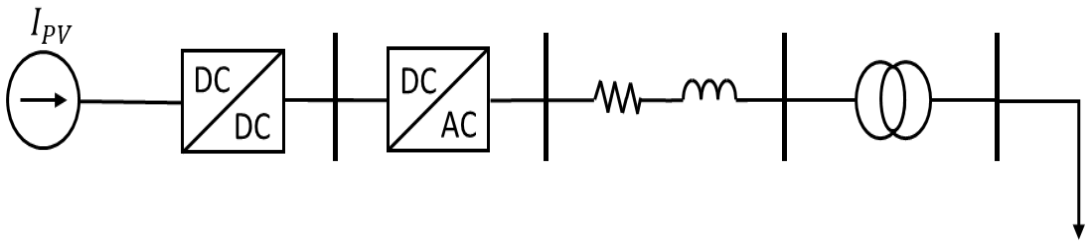

Figure 3.9

PV system single line diagram

Solar cells are the most basic units of a PV module; they directly convert the energy of the photon in the sun light into electric energy by photovoltaic effect. Solar cells are stacked together to form the PV module. To achieve the desired voltage and current, modules are stacked in series and parallel to construct a PV Array. The voltage of the array depends on the number of series connected modules and the current depends on the number of parallel-connected modules.

The DC/DC converter use boost converter to step up the PV-array voltage to an appropriate level based on the magnitude of utility voltage, while the controller of the DC–DC converter is designed to operate as a maximum power point tracker (MPPT) that use the "Perturb and Observe" technique to vary the voltage across the terminals of the PV array in order get the

maximum possible power. The converter is connected to the DC side of the inverter in parallel with a DC capacitor link.

To integrate the PV array's DC output into the power system network it should be converted into an AC quantity. The inverter in the PV system does this job. An inverter is a power electronic converter that converts the DC output of the PV array into grid-compliant AC. The inverter controller compares the AC voltage and frequency of the PV system with a reference values and accordingly regulate the inverter output voltage and frequency.

The amount of output power from a PV system mainly depends on the irradiance and temperature. In this work, these two parameters are assumed to be constant and equal to the standard test conditions, i .e, 1000 W/m^2 for irradiance and 25^o for temperature. Since any transient study is conducted for few seconds then it is reasonable to assume that weather conditions will not change during this small period.

The solar PV generator can be either a single small solar PV power plant, or an equivalent model of mainly distributed solar PV generators. In this work, all the distributed PV plants behind the bus are all aggregated and represented as one equivalent PV generator with one inverter. The number of parallel and series connected modules within the PV array are adjusted to obtain the desired capacity from the PV generator.

3.7 Breaking the algebraic loop

Simulink model for the PV array as shown in figure 3.10 consists of two main parts, which are sunlight insolation dependent current source and diode. The other two elements, namely, shunt resistance R_{SH} and series resistance R_S that adds accuracy to the model.

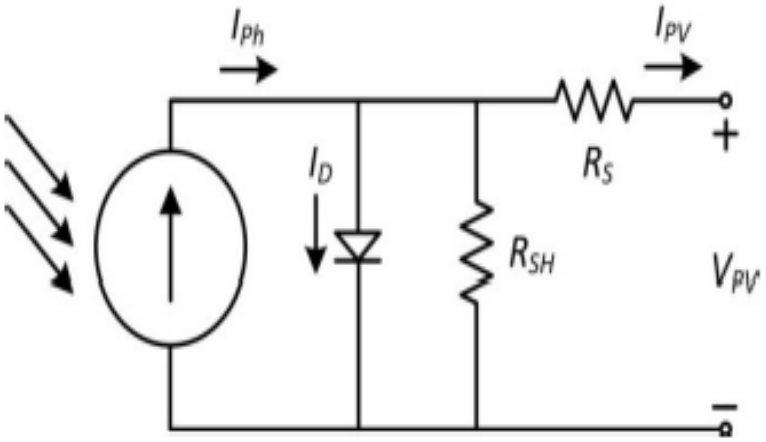

Figure 3.10

PV array model

The diode is also modeled by a controlled current source whose output current is described with Shockley diode equation:

$$I_D = I_0\,(e^{(V_D/n.V_t)} - 1) \qquad 3.1$$

where I_D, I_0, V_D, n and V_t are diode current, diode saturation current, diode voltage, ideality factor and thermal voltage respectively. I_d accounts for the short circuit current of the PV array. From Shockley equation, the diode voltage is used to compute the value of the diode current, this dependency lead to a problem called Algebraic Loop. An algebraic loop generally

occurs when an input port with direct feed through is driven by the output of the same block, either directly, or by a feedback path through other blocks with direct feed through. Direct feedthrough means that Simulink needs the value of the block's input signal to compute its output at the current time step. Such a signal loop creates a circular dependency of block outputs and inputs in the same time-step. This results in an algebraic equation that needs solving at each time-step, adding computational cost to the simulation [31].

This loop is easily solved by Simulink but it cannot be solved by the RT-lab software. So to run the model on the real time platform this loop should be broken. Simulink has an option for the PV array block of breaking this loop, but when selecting this option, the simulation will only work when the step size reduce to very small value, i.e, 1 µs. However, the smallest step size when building and executing any model in RT-lab is 7 µs so this option for breaking the loop will not work for real time simulation.

In order to break this loop a memory block was added (as per the Simulink solution) at the feedback between the voltage measurement and the input signal of the controlled current source that represent the diode. This delay solves the problem of algebraic loop since the value of the state for each step is available from the previous step. Normally adding just this delay would be sufficient to break the algebraic loop, for the array model however, adding the delay doesn't work unless the time step is reduced to be as small as 1 µs. To solve this issue a capacitor was added at the output terminals of the array as shown in figure 3.11 [32] . This capacitor adds a state to the model and solves the step size problem, large step sizes of 40 µs or more could be used. Adding the capacitor influences neither the steady state nor the transient behavior of the PV array because as mentioned above the output of the PV array is a DC voltage.

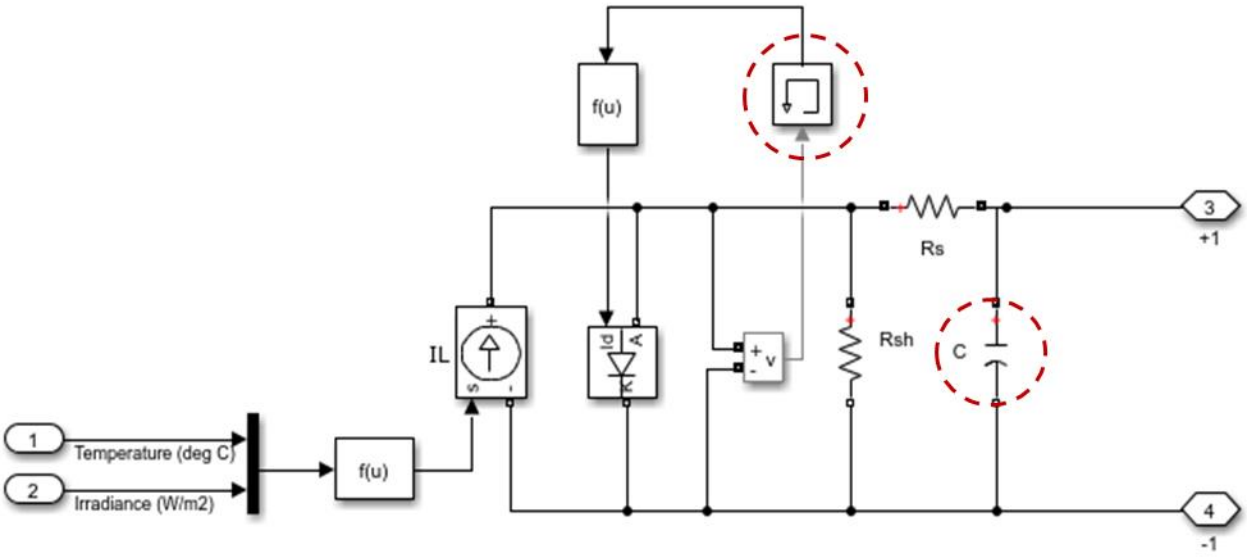

Figure 3.11

PV array model with the loop broken

The capacitor along with the series resistance Rs act as a low pass filter with a time constant of Rs multiplied by C, the value of this time constant is set to be proportional to the simulation step size.

$$R_s \,.\, C \propto T_s$$

Since the value of Rs is constant, the capacitor value should be changed to have the suitable time constant for the used step size. The value of the time constant and accordingly the capacitor should be within a specific range for the particular step size. Selecting a capacitance that is out of this range results in inconsistent output. The minimum time constant ranges from 0.016 s to 0.93 for a step size range of 10 µs to 100 µs. The exact mathematical relation between the time constant and the step size is yet to be found and further research is required.

CHAPTER 4

RESULTS AND DISCUSSION

4.1 Impacts of High PV penetration on transient stability

To study the effect of high PV penetration on the synchronous generators transient stability, a solar PV generator was inserted at each generator bus (except the slack), one at time. Three levels of PV generator penetration were examined: 10%, 25% and 50% of the synchronous machine's MVA. The penetration level refers here is based on the MVA of the SG under study.

In this work, the transient stability was assessed using the critical clearing time (CCT) which was found from the simulation by starting from a small clearing time and observing the rotor angle deviation to see if the system is stable. If stable, then the clearing time is increased and this step repeated until the system loses synchronism at the CCT. Faults applied to each bus were cleared with no coincident loss of element, which assumes an appropriate bus arrangement (e.g., breaker-and-a-half or double-breaker/double-bus).

In order to maintain the power supply-demand balance the output power of the synchronous generator should be decreased as the capacity the PV generator increased. Two methods of decreasing the output power of the synchronous generator were adopted:

4.1.1 PV replaces conventional generation

4.1.1.1 Case I

For this case, the machine MVA and inertia were reduced by a factor, Tables 4.1 and 4.2 show the SG capacity and inertia, respectively, for each PV penetration level.

Table 4.1

SGs' and PV's capacities for different PV penetration levels

Unit	SG Capacity (MVA)				PV Capacity (MVA)			
	0 PV	10% PV	25% PV	50% PV	0 PV	10% PV	25% PV	50% PV
Birch	150	135	112	75	0	15	37	75
Maple U1	100	90	75	50	0	10	25	50
Oak	100	90	75	50	0	10	25	50
Pine	300	270	225	150	0	30	75	150
Maple U2	500	450	375	250	0	50	125	250
Spruce	1000	900	750	500	0	100	250	500

Table 4.2

SGs' inertia for different PV penetration levels

Unit	Inertia (s)			
	0 PV	10% PV	25% PV	50% PV
Birch	9.3	8.4	7	4.7
Maple U1	5.5	4.9	4.1	2.7
Oak	5.5	4.9	4.1	2.7
Pine	10	9	7.5	5
Maple U2	16.2	14.5	12.1	8.1
Spruce	39.6	35.6	29.7	19.8

A solid three-phase fault was applied at the generator step up transformer high side of each SG (one at a time) and the CCT time for each case was found. Figure 4.1 below shows the critical clearing time for each SG when the shown PV levels are injected.

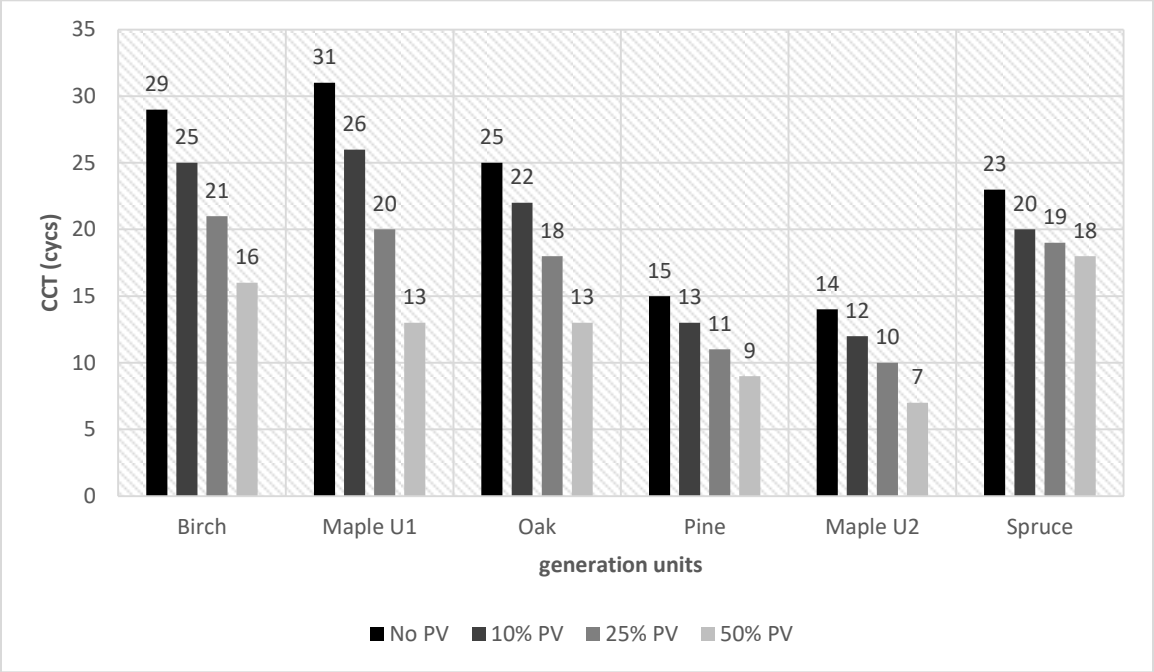

Figure 4.1

CCT for various PV penetration levels

In this case, it is generally observed that increasing photovoltaic penetration level results in an apparent decrease in the critical clearing time for all the synchronous generators and this is mainly due to the reduction of the generator inertia.

4.1.1.2 Case II

For this case, the system has a 25 % PV penetration level, and penetration level referred to in this case is based on the system's total load.

$$25\%\ \text{PV} = 0.25 * \text{total load} = 0.25 * 2100 = 525\ \text{MW}$$

This amount of PV injection was distributed among the SGs as shown in table 4.3 and the capacity of the SG was reduced depending on the amount of the PV generation connected to its bus.

Table 4.3

PV generators distribution for 25% penetration level

Unit	Inertia(s)	SG (MVA)	PV (MVA)
Birch	4.66	75	75
Maple U1	2.74	50	50
Oak	2.74	50	50
Pine	4.99	150	150
Maple U2	9.69	300	200
Spruce	39.59	1000	0

A solid three-phase fault was applied at the generator step-up transformer high side of each SG, one at a time, and the CCT time for each fault was found. Figure 4.2 shows the critical clearing time for each fault location.

4.1.1.3 Case III

For this case, a penetration level of 50% (based on the total load) which is equivalent to 1050 MW was injected to the system; this amount of PV injection was distributed among the

SGs as shown in table 4.4. As in CASE II, the capacity of the SG was reduce depending on the amount of the PV generation connected to its bus.

Table 4.4

PV generators distribution for 50% penetration level

Unit	Inertia(s)	SG (MVA)	PV (MW)
Birch	3.1	50	100
Maple U1	1.4	25	75
Oak	1.4	25	75
Pine	5	150	150
Maple U2	6.5	200	300
Spruce	11.9	650	350

As in case II, a solid three-phase fault was applied at the generator step up transformer high side of each SG. Figure 4.2 shows the critical clearing time for each SG for both cases II and III.

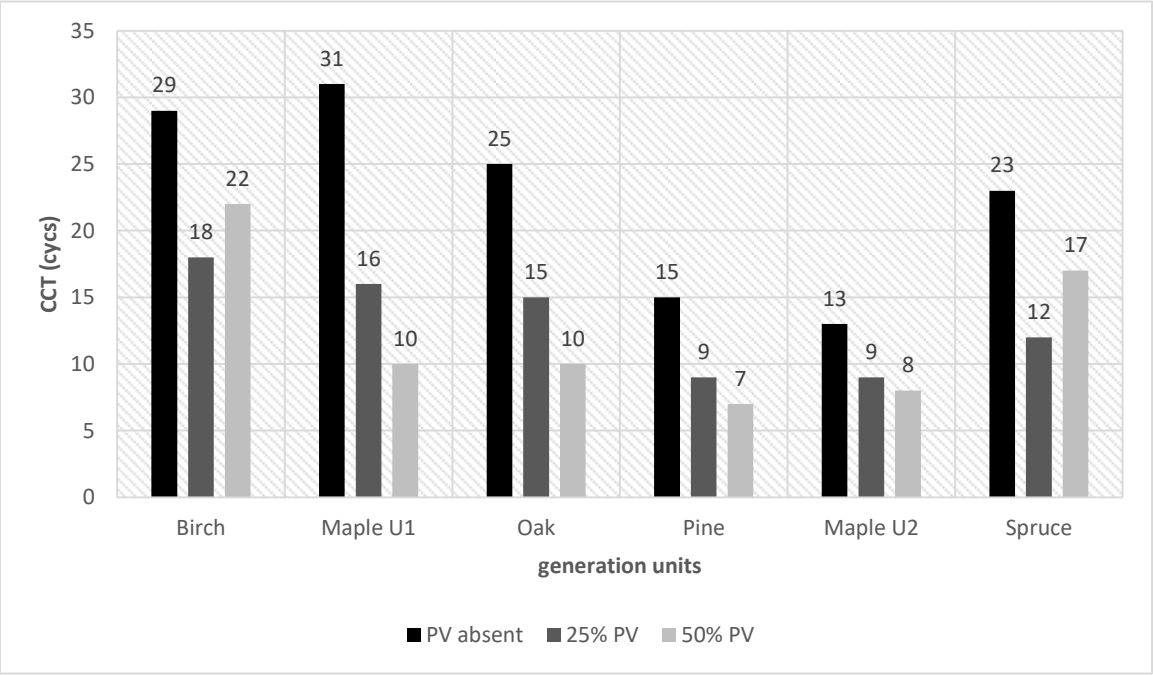

Figure 4.2

CCT for two different PV penetration levels

It can be seen that increasing the PV penetration throughout the system results in a decrease in the CCT for most of the SGs, which is expected since the total system inertia has been reduced, except for the generation units at Birch and Spruce. A probable explanation for this deviation is that having a PV generator in parallel with the SG helps to share part of the fault current which works to improve transient stability. The dynamic response is a complex function that depends on system inertia; fault current contribution of PV and power output, and it is not definite that increasing PV levels will negatively affect transient stability.

4.1.2 PV supplements conventional generation

In the second method of maintain the power supply-demand balance, all the SGs parameters were kept constant and only the reference mechanical power P_{ref} of the governor was reduced to implement the following cases:

4.1.2.1 Case I

In this case the mechanical power P_{ref} of the governor was reduced the by a factor of 0.9, 0.75 and 0.5 to represent the 10%, 25% and 50% penetration levels (based on SG's MVA) respectively. The PV generator with the mentioned capacities was connected to only one SG at a time and a three phase fault was applied at the transformer high voltage side of that SG. Figure 4.3 below shows the critical clearing time for each SG.

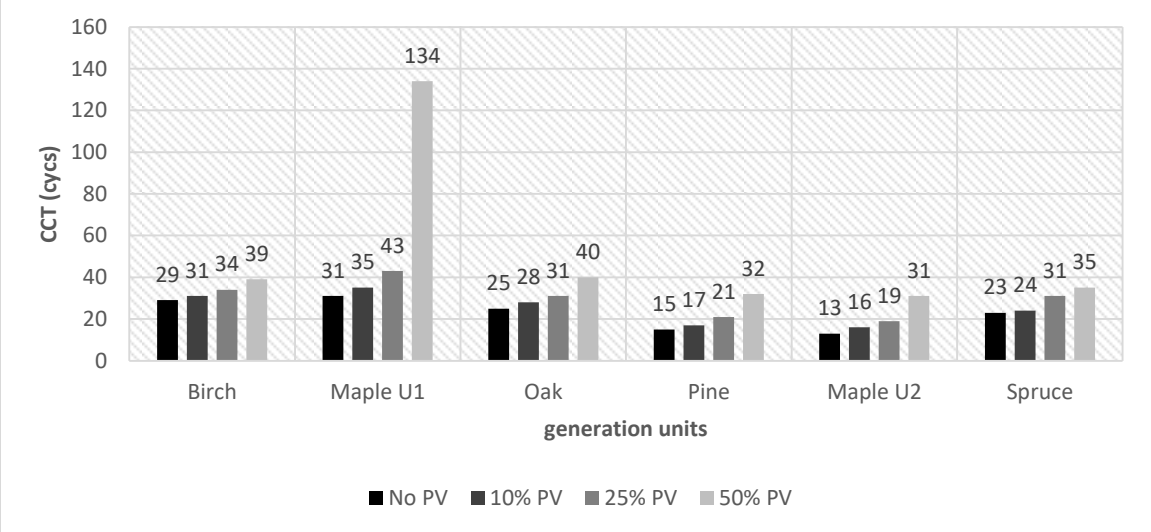

Figure 4.3

CCT for various PV penetration levels

In contrast to the former cases, increasing photovoltaic penetration level in this case leads to an increase in the critical clearing time for all the synchronous generators and this is mainly due to the fact that the generators' inertia and ratings are kept constant while the electrical output power of the generators was reduced.

4.1.2.2 Case II

In this case, the system has a 25 % PV (525 MW) penetration level based on the system's total load. Only the output power of the SGs was reduced depending on the capacity of the PV generator connected with each individual SG.

This amount of PV injection was distributed among the SGs as shown in table 4.3. A solid three-phase fault was applied at the generator step-up transformer high side of each SG, one at a time, and the CCTs are shown in figure 4.4.

4.1.2.3 Case III

Here a penetration level of 50% (based on the total load) which is equivalent to 1050 MW was injected to the system; distribution of PV injection is shown in table 4.4. As in CASE II, only the output of the SG was reduce depending on the amount of the PV generation connected to its bus. A solid three-phase fault was applied at the generator step-up transformer high side of each SG, one at a time, and the CCTs are shown in figure 4.4.

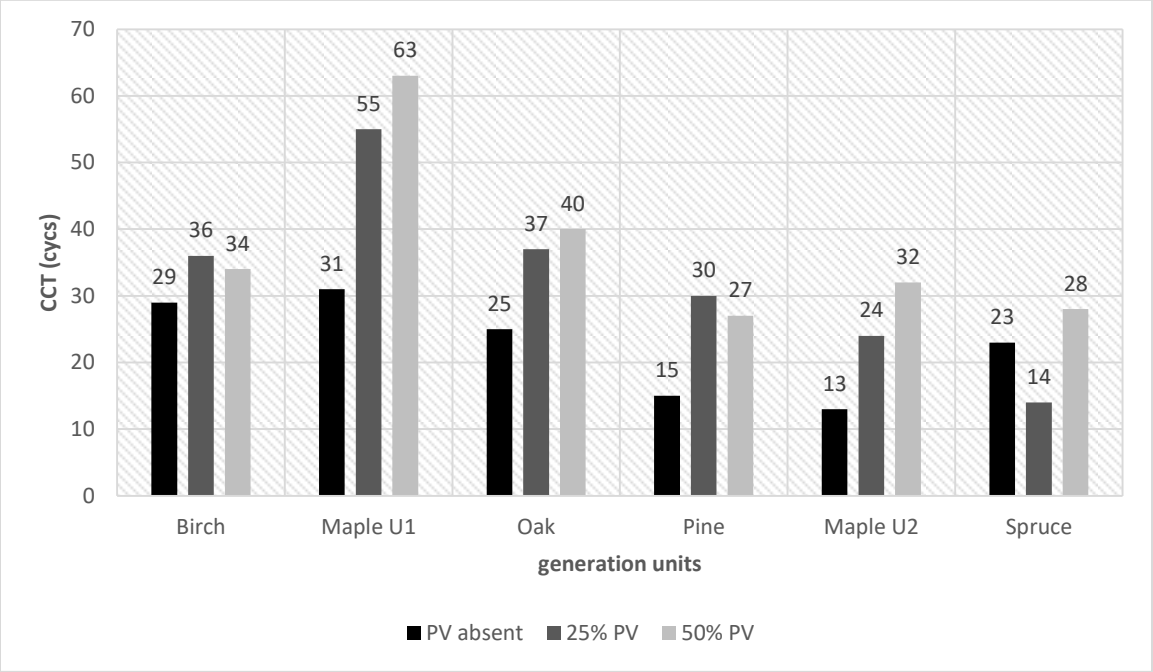

Figure 4.4

CCT for two different PV penetration levels

4.2 Impact of high PV penetration on fault current

To study the impact of high PV penetration on the fault levels, several fault scenarios have been conducted:

4.2.1 CASE I

In this case, each machine capacity has been reduced to half and the other half was replaced by a PV generator. Single line to ground and three phase faults were then applied at the generator step up transformer high-side for each SG (one at a time) for 6 cycles. For the single line to ground faults the neutrals of the high-side of the GSUs and transmission transformers

were grounded. Fault current was measured at the generation bus and compared to the fault current with no PV generator connected with the SG.

Figure 5.5 shows the fault current for a three-phase fault at the generation bus with and without PV injection and Figure 4.6 shows the same comparison for single line to ground type fault. All currents are in pu based on the machine MVA.

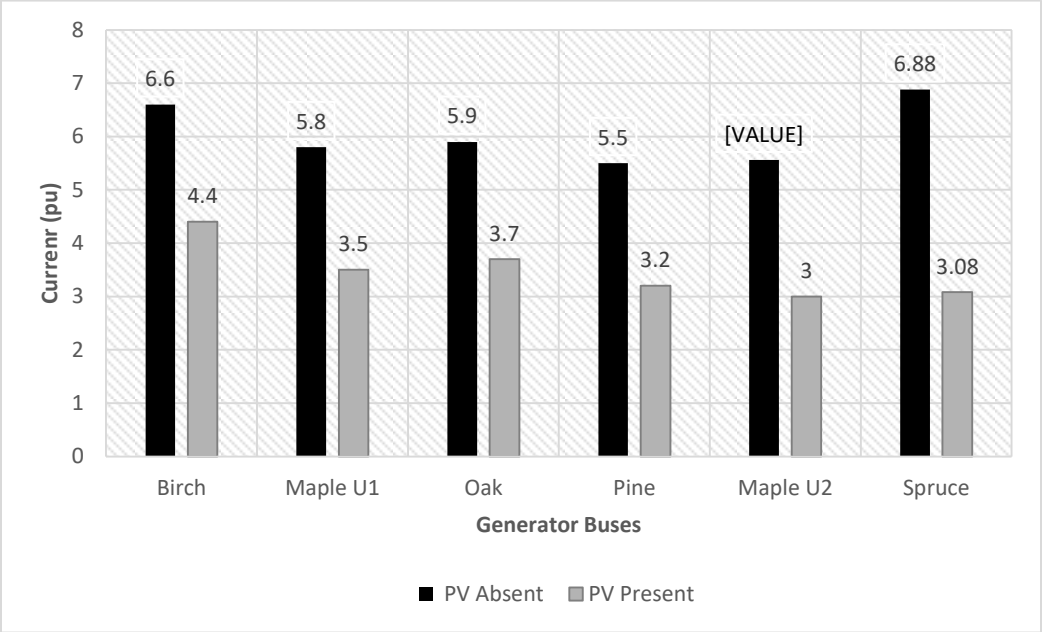

Figure 4.5

Generator Buses Fault Current for 3-ph Fault

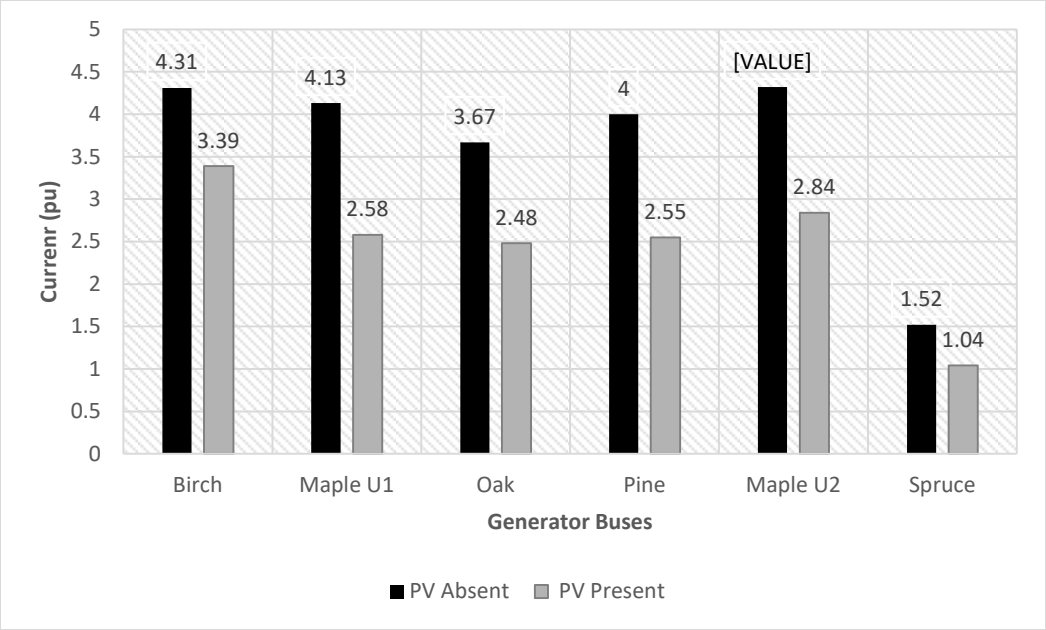

Figure 4.6

Generator Buses Fault Current for SLG Fault

Figure 4.7 below shows PV fault current in pu for the 3-ph and the SLG faults.

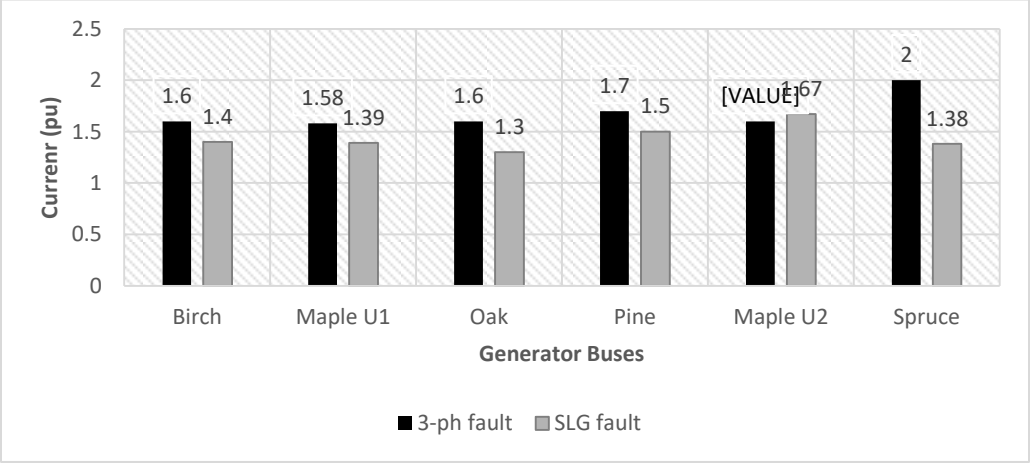

Figure 4.7

PV generator fault current

From figures 4.5 and 4.6 it is clear that replacing part of the SG with a PV generator leads to a significant reduction in the generator bus and consequently the transformer bus currents especially for the three phase fault. This reduction in the fault is caused by the comparatively smaller contribution of the PV generator to the fault current. The PV generator fault current as shown in figure 4.7 is always less than 2 times the inverter rated current because it is governed by the inverter control, which is designed to limit the fault current to 2 times the rated current. The remaining system buses fault current share are not affected since the fault location is at the transformer bus.

4.2.2 CASE II

In this case, the system has a 25 % PV penetration level based on the system's total load which is equivalent to 525 MW from PV generators. This amount of PV injection was distributed among the SGs as shown in table 4.3 and the capacity of the SG was reduced depending on the amount of the PV generation connected to its bus.

Single line to ground and three phase faults were applied for 5 cycles at bus 10. Fault current was measured for all system buses and compared to the fault current without PV generators. Figure 4.7 shows a simplified single line diagram for the system that includes only the buses, generators and indicate the fault location.

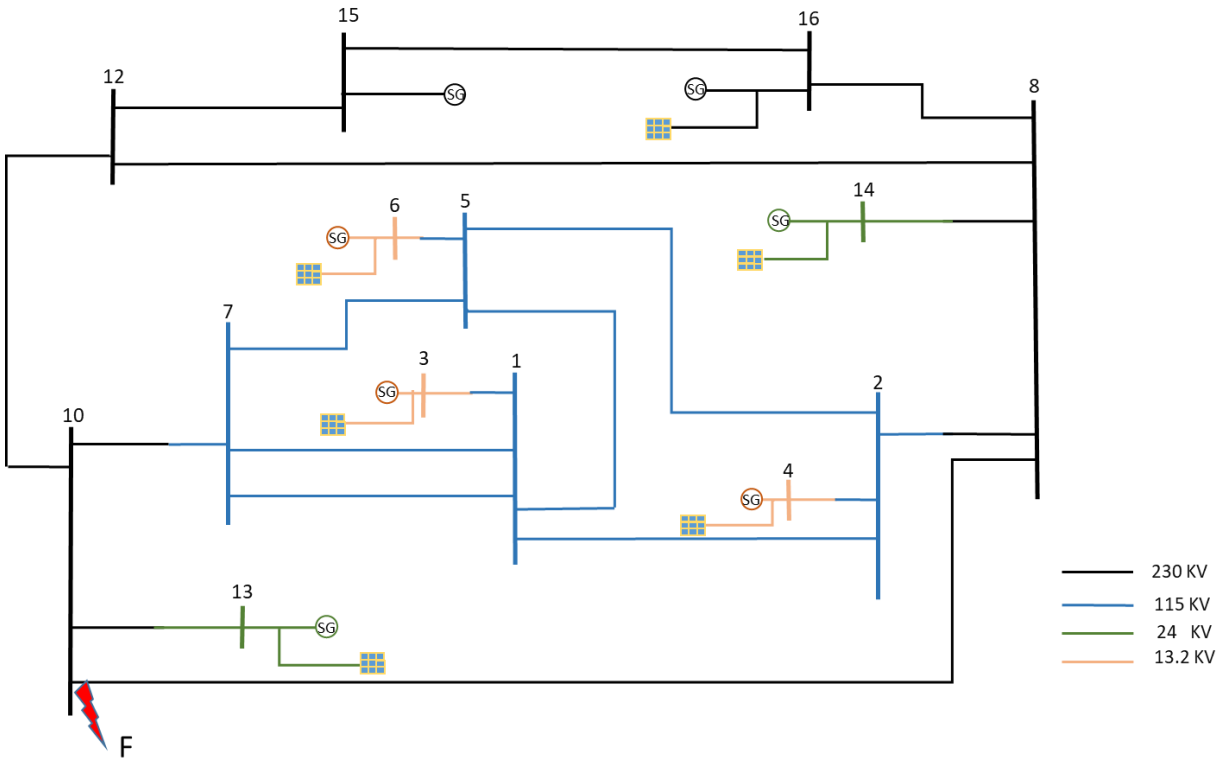

Figure 4.8

3-Ph fault at bus 10

Figure 4.9 and 4.10 represent the percentage of reduction in the total fault current for all system's buses for the three-phase fault and the single line to ground fault respectively.

4.2.3 Case III

In this case, a penetration level of 50%, which is equivalent to 1050 MW was injected to the system, this amount of PV injection was distributed among the SGs as shown in table 4.4 and as in CASE II, the capacity of the SG was reduced depending on the amount of the PV generation connected to its bus.

Single line to ground and three phase faults were applied at bus 10 for 5 cycles. Fault current was measured for all system buses and compared to the fault current without the PV generators. Figure 4.9 shows the percentage of reduction in the fault current for the three-phase fault for case II and case III. Figure 4.10 shows the percentage of reduction in the fault current for the single line to ground fault for case I and case II.

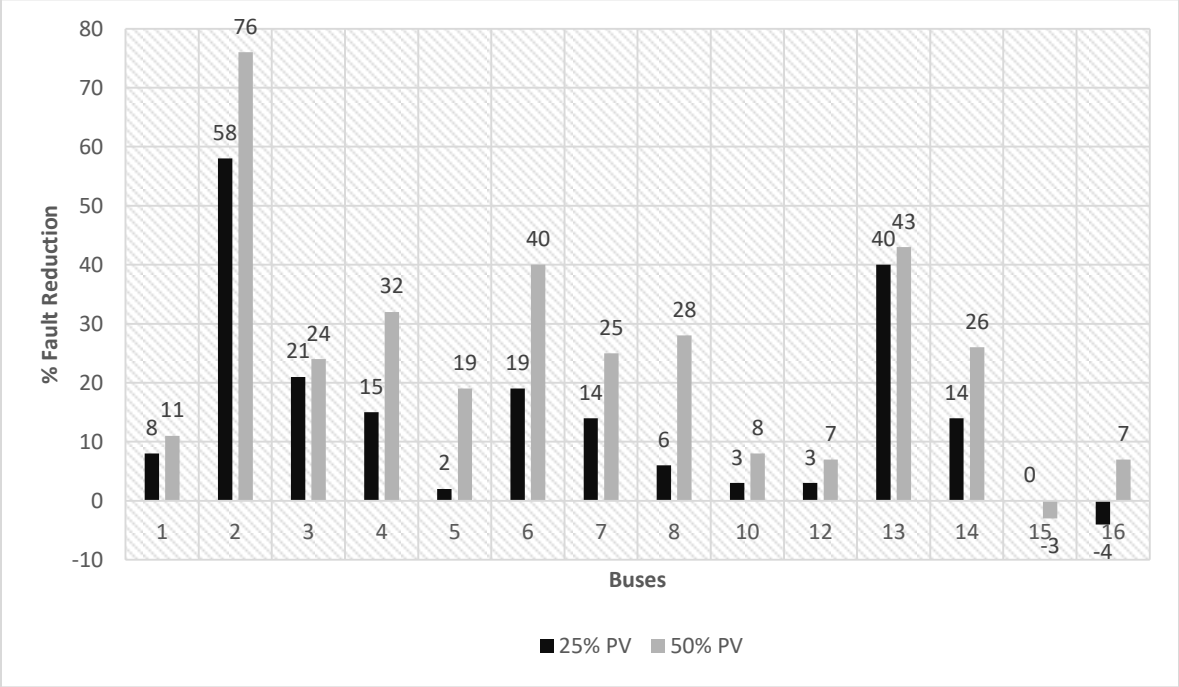

Figure 4.9

Fault current percentage reduction for 3-ph fault

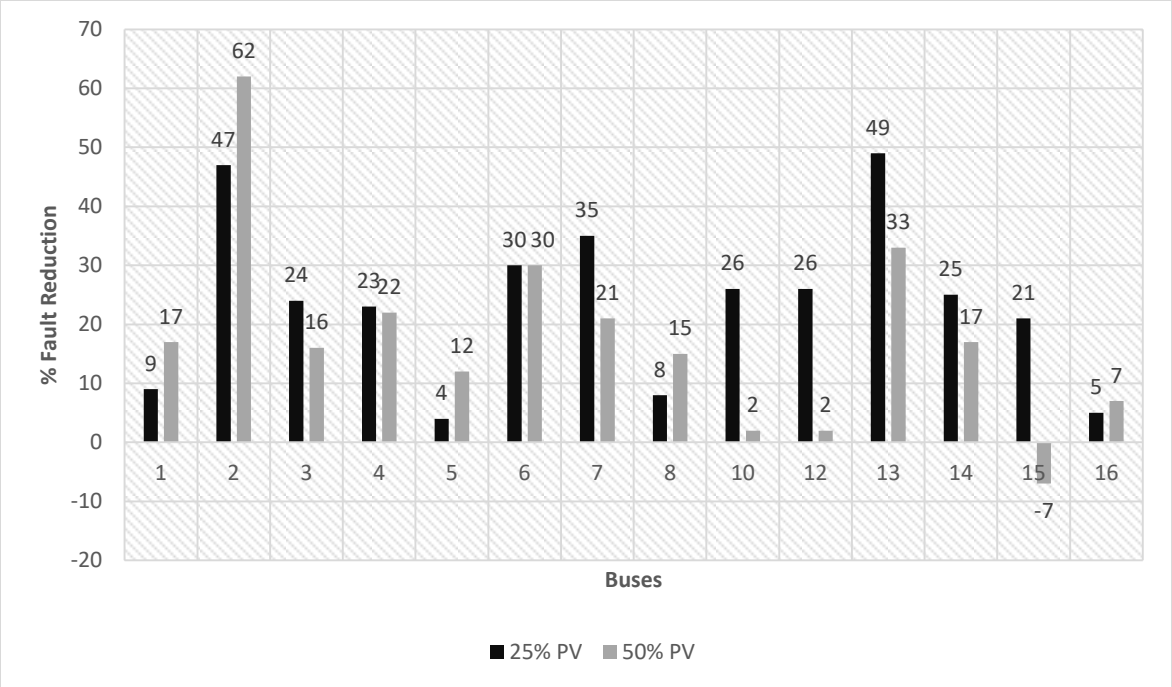

Figure 4.10

Fault current percentage reduction for SLG fault

It can be seen from figure 4.9 that the reduction in the fault current increased as the penetration level increased from 25% to 50%. For the 3 phase fault, the highest decrease in fault current is at bus 2 which connects three generators, where about 75% of their generation was replaced by PV to the fault location, followed by bus 13 which is the closest generator bus to the fault and for which more than half of the SG is replaced by PV generator. The least significant reduction was at the 230 KV buses, namely 10 and 12 whose fault current basically comes from the slack which doesn't have any PV injection. There has been a slight increase in the fault current for bus 15 at which the slack is connected and this due to the fact that the slack increased its output power slightly when connecting the PV generation to supplement the gap in the power since the PV generators efficiency is less than 100%. For the single line to ground fault the

reduction in the fault current is also significant for most of the buses. To sum up, PV penetration does not reduce fault by the same amount along the system, the reduction depends on the distribution of the PV generation, the fault type and location with respect to the PV generators.

4.2.4 Case IV

In this case, the system has a 25 % PV penetration level based on the system's total load and it is distributed as shown in table 4.3. In this case the parameters of the SGs were left unchanged and only the output of the SGs was reduced according to the amount of PV connected. A three phase fault was applied for 5 cycles at bus 10. Fault current was measured for all system buses and compared to the fault current without PV generators as shown in figure 4.11

4.2.5 Case V

In this case, a penetration level of 50%, which is equivalent to 1050 MW was injected to the system and it is distributed as shown in table 4.4 and as in CASE II, the capacity of the SGs was left unchanged and the output power for each SG was cut down depending on the amount of the PV generation connected to its bus. A three phase fault was applied at bus 10 for 5 cycles. Fault current was measured for all system buses and compared to the fault current without the PV generators. Figure 4.11 shows the percentage of reduction in the fault current for cases IV and V.

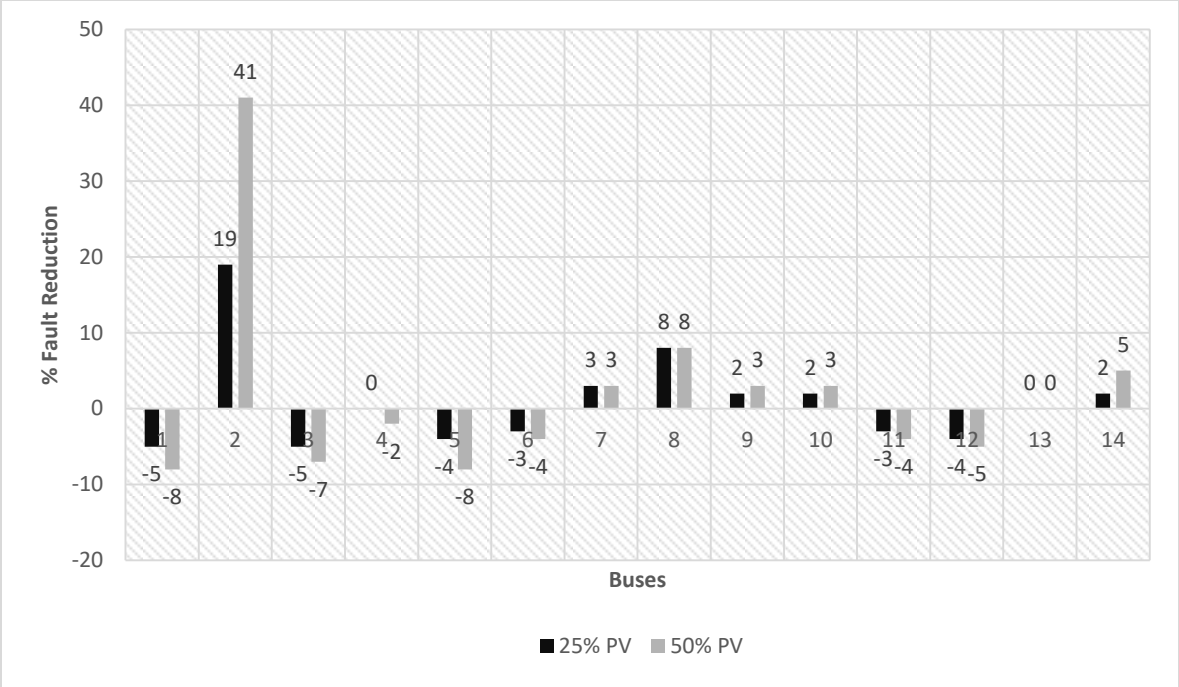

Figure 4.11

Fault current percentage reduction for 3-ph fault

In case IV and V the fault current increased for some buses and decreased for other. For almost all buses either the reduction or the increase was less than 10%.

CHAPTER 5

CONCLUSION AND FUTURE WORK

5.1 Conclusion

In this work, the effect of high penetration levels of solar photovoltaic on synchronous generators transient stability and fault current was studied. It was found that dividing the generation between SGs and PVs could enhance or degrade the SGs' transient stability depending on the machine's inertia, fault levels and power settings. If the inertia is kept unchanged, representing PV that supplements rather than replaces SG, the transient stability performance will be enhanced and the critical clearing time will increase as the penetration level increase. In contrast, reducing the inertia (where PV replaces SG) negatively affects the transient stability and the critical clearing time generally decreases as the penetration level increase. However, this is not always the case, and there may be some situations where increasing PV penetration actually improves the critical clearing times.

It was found that high level injections of PV where PV replaces SG results in a significant reduction in the fault current because the fault current contribution of the PV generator does not exceed 2 times the inverter rating current unlike the SGs. This reduction depends on the penetration level and the allocation of the PV generators along the system. It also depends on the fault type and location.

A PV generator model that can work on real-time digital simulators environment was developed by breaking the algebraic loop of the old model. It was found necessary to both add

memory and a capacitor to the PV model to arrive at a working model for the PV for the selected time step. This is in contrast to previous efforts, which recommend one or the other. The capacitor range was determined experimentally.

5.2 Future Work

It would be constructive to investigate the exact mathematical relation between the simulation step size and the capacitance that is added to break the algebraic loop. It would also be useful to apply the methods developed in this work and conduct actual Hardware-In-The Loop tests to examine the effects of large-scale PV penetration on the operation of microprocessor relays specifically for transmission line protection.

REFERENCES

[1] Poolla, B. Kameshwar, S. Bolognani and F. Dörfler, "Optimal Placement of Virtual Inertia in Power Grids," IEEE Transactions on Automatic Control, p. 12, 2017.

[2] "Federal Energy Management Program. Executive Order 13693—Planning for Federal Sustainability in the Next Decade.," 25 March 2015. [Online]. Available: https://www.gpo.gov/fdsys/pkg/FR-2015-03-25/ pdf/2015-07016.pdf. [Accessed 15 May 2020].

[3] J. Keller and B. Kroposki, "Understanding fault characteristics of inverter-based distributed energy resources," NREL, Colorado,USA, 2010.

[4] Pokharel, S. Prasad, Brahma, S. M., Ranade and S. J., "Modeling and simulation of three phase inverter for fault study of microgrids," in 2012 North American Power Symposium (NAPS), Champaign, IL, 2012.

[5] P. Kundur, N. J. Balu and M. G. Lauby, Power system stability and control, New York: McGraw-hill, 1994.

[6] Baran, M.E. and El-Markaby, "Fault Analysis on Distribution Feeders with DG," in IEEE Transaction, 2005.

[7] "IEEE Approved Draft Guide to Conducting Distribution Impact Studies for Distributed Resource Interconnection," IEEE P1547.7/D11, June 2013, pp. 1-129, 2014.

[8] Dugan, Zavadil and V. Holde, "Interconnection Guidelines for Distributed Generation," 2002.

[9] Barker and d. Mello, "Determining the Impact of DG on Power Systems: Part 1 – Radial Distribution System," in Power Technologies, 2000.

[10] al. and G. J. B. et, "Static power converters of 500 kW or less serving as the relay interface package for nonconventional generators," IEEE Transactions on Power Delivery, vol. 9, pp. 1325-1331, 1994.

[11] Development and G. C. Research, "DG Power Quality, Protection and Reliability Case Studies Report," National Renewable Energy Laboratory, Golden, CO, 2003.

[12] Mello, P. P. Barker and R. W. De, "Determining the impact of distributed generation on power systems. I. Radial distribution systems," in 2000 Power Engineering Society Summer Meeting (Cat. No.00CH37134), 2000, pp. 1645-1656 vol. 3.

[13] Brahma, A. Girgis and S., "Effect of distributed generation on protective device coordination in distribution system," in LESCOPE 01. 2001 Large Engineering Systems Conference on Power Engineering. Conference Proceedings. Theme: Powering Beyond 2001 (Cat. No.01ex490), 2001, pp. 115-119.

[14] M. Akmal, F. Al-Naemi, N. Iqbal, A. Al-Tarabsheh and L. Meegahapola, "Impact of Distributed PV Generation on Relay Coordination and Power Quality," in 2019 IEEE Milan PowerTech, 2019, pp. 1-6.

[15] Nour, R. R. Waqfi and M., "Impact of PV and wind penetration into a distribution network using Etap," in 2017 7th International Conference on Modeling, Simulation, and Applied Optimization (ICMSAO), 2017, pp. 1-5.

[16] K. R, Komor and A. Hoke, "Smart Grids and Renewables," IRENA, Colorado, 2013.

[17] S. Bhattacharya, T. Saha and M. J. Hossain, "Fault current contribution from photovoltaic systems in residential power networks," in 2013 Australasian Universities Power Engineering Conference (AUPEC), 2013, pp. 1-6.

[18] P. al and K. et, "Definition and classification of power system stability IEEE/CIGRE joint task force on stability terms and definitions," IEEE Transactions on Power Systems, vol. 19, pp. 1387-1401, 2004.

[19] D. Hill, I. Hiskens and D. Popovic, "Load recovery in voltage stability analysis and control," Proc. NSF/ECC Workshop on Bulk Power System Voltage Phenomena, pp. 579-595, 1994.

[20] Tamura, M. Yagami and J., "Impact of high-penetration photovoltaic on synchronous generator stability," in 2012 XXth International Conference on Electrical Machines, IEEE, 2012, pp. 2092-2097.

[21] M. Z. C. Wanik, I. Erlich, A. Mohamed and A. A. Salam, "Influence of distributed generations and renewable energy resources power plant on power system transient stability," in 2010 IEEE International Conference on Power and Energy, IEEE, 2010, pp. 420-425.

[22] S. R. Mohamed, P. A. Jeyanthy and D. Devaraj, "Investigation on the impact of high-penetration of PV generation on transient stability," in 2017 IEEE International Conference on Intelligent Techniques in Control, Optimization and Signal Processing (INCOS), IEEE, 2017, pp. 1-6.

[23] W. Yi, D. J. Hill and Y. Song, "Impact of High Penetration of Renewable Resources on Power System Transient Stability," in 2019 IEEE Power Energy Society General Meeting (PESGM), IEEE, 2019, pp. 1-5.

[24] D. S. Kumar, A. Sharma, D. Srinivasan and T. Reindl, "Impact analysis of large power networks with high share of renewables in transient conditions," IET Renewable Power Generation, vol. 14, pp. 1349-1358, 2020.

[25] Kaygusuz, O. Tuttokmagi and A., "Transient Stability Analysis of a Power System with Distributed Generation Penetration," in 2019 7th International Istanbul Smart Grids and Cities Congress and Fair (ICSG), IEEE, 2019, pp. 154-158.

[26] Z. Liu, Z. Zhang and Y. Lin, "Impact of Inverter-Interfaced Renewable Generation on Transient Stability at Varying Levels of Penetration," in IECON 2018 - 44th Annual Conference of the IEEE Industrial Electronics Society, IEEE, 2018, pp. 4027-4032.

[27] "Mathworks," [Online]. Available: https://www.mathworks.com/help/physmod/sps/powersys/ref/synchronousmachine.htm.

[28] "IEEE Recommended Practice for Excitation System Models for Power System Stability Studies - Redline," IEEE Std 421.5-2016 (Revision of IEEE Std 421.5-2005) - Redline, pp. 1-453, 2016.

[29] K. Padiyar, Power system dynamics, BS publications, 2008.

[30] I. C. Report, "Dynamic Models for Steam and Hydro Turbines in Power System Studies," IEEE Transactions on Power Apparatus and Systems, Vols. PAS-92, pp. 1904-1915, 1973.

[31] "Mathworks," [Online]. Available: https://www.mathworks.com/help/simulink/ug/algebraic-loops.html.

[32] S. Arash, " modeling, analysis, and design of a pv-based grid-tied plug-in hybrid electric vehicle battery pack charger," Montréal, Québec, Canada, 2013.

VITA

Amira Abdelgadir was born in Khartoum, Sudan in 1994. In 2016, she earned her Bachelor of Science (Honors) in Electrical and Electronic Engineering with First Class at the University of Khartoum, Sudan. After graduation, she worked as a teaching assistant at the University of Khartoum until she was awarded a graduate assistantship, in August 2018, from the University of Tennessee at Chattanooga to pursue her master's degree in Electrical Engineering.